

Artificial intelligence and machine learning for medical imaging: a technology review

Ana Barragán-Montero^{1*}, Umair Javaid¹, Gilmer Valdés², Dan Nguyen³, Paul Desbordes⁴, Benoit Macq⁴, Siri Willems⁵, Liesbeth Vandewinckele⁶, Mats Holmström⁷, Fredrik Löfman⁷, Steven Michiels¹, Kevin Souris¹, Edmond Sterpin^{1,6}, John A. Lee¹

¹Molecular Imaging, Radiation and Oncology (MIRO) Laboratory, UCLouvain

²Department of Radiation Oncology, Department of Epidemiology and Biostatistics, University of California, San Francisco

³Medical Artificial Intelligence and Automation (MAIA) Laboratory, Department of Radiation Oncology, UT Southwestern Medical Center

⁴Information and Communication Technologies, Electronics and Applied Mathematics (ICTEAM), UCLouvain

⁵ESAT/PSI, KU Leuven Belgium & MIRC, UZ Leuven, Belgium

⁶KU Leuven, Department of Oncology, Laboratory of Experimental Radiotherapy

⁷RaySearch Laboratories AB

*corresponding author

Abstract

Artificial intelligence (AI) has recently become a very popular buzzword, as a consequence of disruptive technical advances and impressive experimental results, notably in the field of image analysis and processing. In medicine, specialties where images are central, like radiology, pathology or oncology, have seized the opportunity and considerable efforts in research and development have been deployed to transfer the potential of AI to clinical applications. With AI becoming a more mainstream tool for typical medical imaging analysis tasks, such as diagnosis, segmentation, or classification, the key for a safe and efficient use of clinical AI applications relies, in part, on informed practitioners. The aim of this review is to present the basic technological pillars of AI, together with the state-of-the-art machine learning methods and their application to medical imaging. In addition, we discuss the new trends and future research directions. This will help the reader to understand how AI methods are now becoming an ubiquitous tool in any medical image analysis workflow and pave the way for the clinical implementation of AI-based solutions.

50 **1. Introduction**

1 51

2 52 For the last decade, the locution *Artificial Intelligence* (AI) has progressively flooded many
3 53 scientific journals, including those of image processing and medical physics. Paradoxically,
4 54 though, AI is an old concept, starting to be formalized in the 1940s, while the term of artificial
5 55 intelligence itself was coined in 1956 by John McCarthy. In short, AI refers to computer
6 56 algorithms that can mimic features that are characteristic of human intelligence, such as
7 57 problem solving or learning. The latest success of AI has been made possible thanks to
8 58 tremendous growths of both computational power and data availability. In particular, AI
9 59 applications based on machine learning (ML) algorithms have experienced unprecedented
10 60 breakthroughs during the last decade in the field of computer vision. The medical community
11 61 has taken advantage of these extraordinary developments in order to build AI applications that
12 62 get the most of medical images, automating different steps of the clinical practice or providing
13 63 support for clinical decisions. Papers relying on AI and ML report promising results in a wide
14 64 range of medical applications [1–7]. Disease diagnosis, image segmentation or outcome
15 65 prediction are some of the tasks that are experiencing a disruptive transformation thanks to
16 66 the latest progress of AI.

17 67

18 68 More recently, ML tools have become mature enough to fulfill clinical requirements and, thus,
19 69 research and clinical teams, as well as companies are working together to develop clinical AI
20 70 solutions. Today, we are closer than ever to the clinical implementation of AI and, therefore,
21 71 getting to know the basics of this technology becomes a “must” for every professional in the
22 72 medical field. Helping the medical physics community to acquire such a solid background
23 73 knowledge about AI and learning methods, including their evolution and current state of the
24 74 art, will certainly result in higher quality research, facilitate the first steps of new researchers
25 75 in this field, and inspire novel research directions.

26 76

27 77 The goal of this review article is to briefly walk the reader through some basic AI concepts with
28 78 focus on medical imaging processing (Section 2); followed by a presentation of the state-of-
29 79 the-art methods and current trends in the domain (Section 3). To finish, we discuss the future
30 80 research directions that will make possible the next generation of AI-based solutions for
31 81 medical image applications (Section 4).

32 82

33 83

34 84 **2. Building blocks of AI methods for medical imaging**

35 85

36 86 The field of AI evolves rapidly, with new methods published at a high pace. However, there
37 87 are several central concepts that have settled for good. This section presents a brief overview
38 88 of these building blocks for AI methods, with a focus on medical imaging. For more detailed
39 89 descriptions we refer to relevant books [8–11] and publications [12,13].

40 90

41 91 **2.1. Artificial intelligence, machine learning, and deep learning**

42 92

43 93 As mentioned previously, AI broadly refers to any method or algorithm that mimics human
44 94 intelligence. Historically, AI has been approached from two directions: computationalism and
45 95 connectionism. The former attempts to mimic formal reasoning and logic directly, regardless
46 96 of its biological implementation. Mostly based on hardcoded axioms and rules that are
47 97 combined to deduce new conclusions, computationalism is conceptually similar to computers,

48 98

49 99

50 100

51 101

52 102

53 103

54 104

55 105

56 106

57 107

58 108

59 109

60 110

61 111

62 112

63 113

64 114

65 115

66 116

67 117

68 118

69 119

70 120

71 121

72 122

73 123

74 124

75 125

76 126

77 127

78 128

79 129

80 130

81 131

82 132

83 133

84 134

85 135

86 136

87 137

88 138

89 139

90 140

91 141

92 142

93 143

94 144

95 145

96 146

97 147

98 148

99 149

100 150

101 151

102 152

103 153

104 154

105 155

106 156

107 157

108 158

109 159

110 160

111 161

112 162

113 163

114 164

115 165

116 166

117 167

118 168

119 169

120 170

121 171

122 172

123 173

124 174

125 175

126 176

127 177

128 178

129 179

130 180

131 181

132 182

133 183

134 184

135 185

136 186

137 187

138 188

139 189

140 190

141 191

142 192

143 193

144 194

145 195

146 196

147 197

148 198

149 199

150 200

151 201

152 202

153 203

154 204

155 205

156 206

157 207

158 208

159 209

160 210

161 211

162 212

163 213

164 214

165 215

166 216

167 217

168 218

169 219

170 220

171 221

172 222

173 223

174 224

175 225

176 226

177 227

178 228

179 229

180 230

181 231

182 232

183 233

184 234

185 235

186 236

187 237

188 238

189 239

190 240

191 241

192 242

193 243

194 244

195 245

196 246

197 247

198 248

199 249

200 250

201 251

202 252

203 253

204 254

205 255

206 256

207 257

208 258

209 259

210 260

211 261

212 262

213 263

214 264

215 265

216 266

217 267

218 268

219 269

220 270

221 271

222 272

223 273

224 274

225 275

226 276

227 277

228 278

229 279

230 280

231 281

232 282

233 283

234 284

235 285

236 286

237 287

238 288

239 289

240 290

241 291

242 292

243 293

244 294

245 295

246 296

247 297

248 298

249 299

250 300

251 301

252 302

253 303

254 304

255 305

256 306

257 307

258 308

259 309

260 310

261 311

262 312

263 313

264 314

265 315

266 316

267 317

268 318

269 319

270 320

271 321

272 322

273 323

274 324

275 325

276 326

277 327

278 328

279 329

280 330

281 331

282 332

283 333

284 334

285 335

286 336

287 337

288 338

289 339

290 340

291 341

292 342

293 343

294 344

295 345

296 346

297 347

298 348

299 349

300 350

301 351

302 352

303 353

304 354

305 355

306 356

307 357

308 358

309 359

310 360

311 361

312 362

313 363

314 364

315 365

98 storing and processing symbols. Connectionism, on the other hand, rather follows a bottom-
 1 99 up approach, starting from models of biological neurons that are interconnected in large
 2 100 numbers and from which intelligence is intended to emerge by learning from experience.
 3 101 Expert systems [14–16], which started to be very popular in the 1980, are a classical example
 4 102 of computationalism. Some famous applications of expert systems to the medical field are
 5 103 MYCIN (diagnosis of bacterial infection in the blood) [17], PUFF (interpretation of pulmonary
 6 104 function data) [18], or INTERNIST-1 (diagnosis for internal medicine) [19]. However, the
 7 105 bottleneck of expert systems is the complexity of acquiring the required knowledge in the form
 8 106 of production rules and, thus, interest in computationalist algorithms started to fade since the
 9 107 1990's in favor of connectionism approaches [20,21]. The appeal of connectionism and
 10 108 learning-based AI holds in that it delegates the responsibility for accuracy and exhaustiveness
 11 109 to data instead of human experts, who might be poorly available, prone to error, bias, or
 12 110 subjectivity. The ever growing abundance of data, including medical images, then typically tilts
 13 111 the scales in favor of learning techniques, and the community has focused successively on
 14 112 two nested subfamilies (Figure 1): machine learning and deep learning.
 15 113

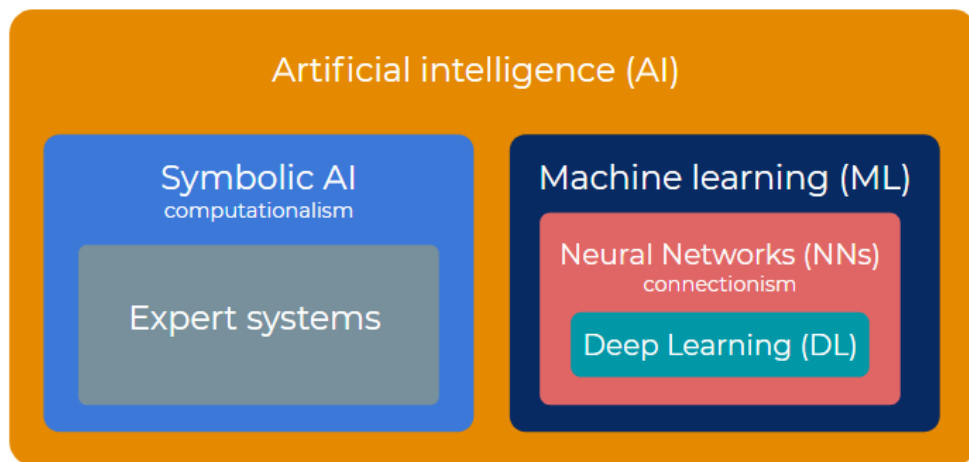


Figure 1. Artificial intelligence, machine learning, and deep learning can be seen as matryoshkas nested in each other. Artificial intelligence gathers both symbolic (top down) and connectionist (bottom up) approaches. Machine learning is the dominant branch of connectionism, combining biological (neural networks) and statistical (data-driven learning theory) influences. Deep learning focuses mainly on large-size neural networks, with functional specificities to process images, sounds, videos, etc.

114
 115 The specificity of Machine learning (ML) is to be driven by data, which gives machines
 116 (computers) “the ability to learn without being explicitly programmed”, as formulated by Arthur
 117 Samuel in 1959, a pioneer in the ML field. ML typically works in two phases, training and
 118 inference. Training allows patterns to be found in previously collected data, whereas inference
 119 compares these patterns to new unseen data to then carry out a certain task like prediction or
 120 decision making. Since the 1990's, ML algorithms have continuously evolved and improved,
 121 becoming more sophisticated and including hierarchical structures, which gave rise to the
 122 popular Deep Learning. The term Deep Learning (DL) was first coined by Aizenberg et al.[22]
 123 in the 2000s, and refers to a subset of ML algorithms, with the particularity of being organized

124 hierarchically, on multiple levels, hence the term “deep”, to automatically extract meaningful
125 features from data.

126 Although ML encompasses DL, DL is often opposed to classical “shallow” ML, the latter relying
127 on algorithms that have a flatter architecture and depend on previous feature engineering to
128 extract data representations. This distinction also reflects the evolution from ML to DL, namely,
129 from specific feature engineering to generic feature learning. While ML generally relies on
130 domain knowledge and expertise to define relevant features, DL involves generic, trainable
131 features. In other words, despite the modeling power of ML, global performance remains
132 limited by the adequacy of manually picked features. Alternatively, DL replaces these fixed
133 specialized features with generic, trainable, low-level features that are involved in the learning
134 procedure, thereby offering better performance guarantees. Sophistication is here achieved
135 by stacking layers of simple features, leading to a hierarchical model structure. As training in
136 DL concerns both the low-level features and the higher-level model, DL is often referred to as
137 an *end-to-end* approach. For image data, this approach typically allows DL to learn optimal
138 filters.

139 Today, ML models have reached important milestones, in some cases being able to
140 accomplish tasks with an accuracy that is similar to or even better than human experts. For
141 instance, the diagnostic performance of DL models has demonstrated to be equivalent to that
142 of health-care professionals for certain applications [23], such as skin-cancer detection [24] or
143 breast cancer detection [25]. In particular, the latter reported a DL model that not only reached
144 an excellent performance in mammogram classification, but also outperformed five out of five
145 full-time breast-imaging specialists with an average increase in sensitivity of 14% [25]. Image
146 segmentation is another task that has experienced a transformation with the advent of ML
147 algorithms. For instance, a recent study has described a DL model that can perform organ
148 segmentation in the head and neck region from CT images with performance comparable to
149 experienced radiographers [26]. For more detailed examples of the performance of state-of-
150 the-art ML and DL methods for medical applications we refer to Section 3.

151

152

153 **2.2. Learning frameworks and strategies**

154

155 Machine learning can be broadly split into two complementary categories, supervised and
156 unsupervised, which are inspired from human learning (Table 1). Supervised learning is the
157 simplest and provides the tightest framework with strongest guarantees. It formalizes learning
158 with a parent or teacher, providing the inputs and controlling the outputs. In supervised
159 learning, the training data consists thus of labelled or annotated (input,output) pairs, and the
160 model is trained to yield the right desired output when presented with some input. When data
161 is not annotated, unsupervised learning, also known as self-organization, aims at discovering
162 patterns in data (Figure 2).

163

164 Typical supervised tasks involve function approximation, like regression and classification.
165 Classification can be binary, like in determining whether a pathology is present or not in an
166 image [25,27], involve multiple classes, as in determining a particular pathology among
167 several labels [28–30], or concern not the whole image but each pixel, as done for image
168 segmentation [31,32]. On the regression side, also in a pixel-wise way, image enhancement
169 (e.g. improving a low-quality image, the input, by mapping it to its higher quality counterpart,
170 the output label or annotation) [33] or image-to-image mapping (e.g. mapping a CT image, the
171 input, to the corresponding dose distribution, the output) [34]. More examples of clinical

172 applications of supervised learning and the common ML methods used within this learning
173 framework are presented in Table 1.

174
175 In contrast, most unsupervised tasks relate to probability density estimation, like clustering
176 (finding separated groups of similar data items), outlier or anomaly detection (isolated items),
177 or even manifold learning and dimensionality reduction (subspaces on which data
178 concentrate). The use of unsupervised learning has been, so far, much more limited than its
179 supervised counterpart, although useful applications for medical imaging exist, such as
180 domain adaptation (e.g., adapting a segmentation model trained on an image modality to work
181 on a different image modality) [35–37], data generation (e.g., generate artificial realistic
182 images) [38–40] or even image segmentation [41]. Table 1 presents some of the main ML
183 methods that work in an unsupervised framework.

184
185 Semi-supervised learning is a hybrid framework halfway between supervised and
186 unsupervised and thus it involves data for which desired outputs are only partly known. Groups
187 identified as clusters by unsupervised learning can be used as possible class labels [42]
188 (Figure 2). Some examples of clinical applications for semi-supervised learning include the
189 generation or translation of images from a specific class to another in a semi-supervised
190 setting (e.g., generation of synthetic CTs from MR images) [43,44], and segmentation or
191 classification of images with partially labelled data [45,46].

192
193 So far, supervised learning has been the most used learning framework for medical imaging
194 applications, as it is totally univocal and models are very easy to train. However, it is well-
195 known that data labelling in the medical domain is an extremely time-consuming task, subject
196 to costly inspection by human experts. Therefore, more and more researchers are now
197 exploring semi-supervised learning techniques because they are an excellent alternative to
198 complement small sets of carefully labelled data with large amounts of cheap unlabelled data
199 collected automatically [42,47]. In fact, many of the current limitations of ML/DL algorithms
200 come from the use of labelled data (e.g., errors in labels [48], limited size labelled databases,
201 etc) and thus, although the use of fully unsupervised learning in the medical field is still very
202 limited, we believe that future research will focus on unsupervised techniques in order to
203 unlock the full potential of ML. Very recently, unsupervised models are achieving improved
204 performances over supervised models for computer vision tasks [49], and the same is likely
205 to happen for medical imaging applications.

206
207 Yet another type of learning is by interacting with an environment where an agent gets
208 feedback from its actions over the course of time, which is known as reinforcement learning.
209 After each action towards a new state, the environment can either reward or punish the agent
210 who has then to best predict the longer-term consequences of future actions in a trial and error
211 fashion. The use of reinforcement learning for medical imaging is still not very extended, but
212 has increased in the last couple of years, with promising applications that allow mimicking
213 physician behaviour for typical tasks such as the design of a treatment [50–55], among others
214 (Table 1).

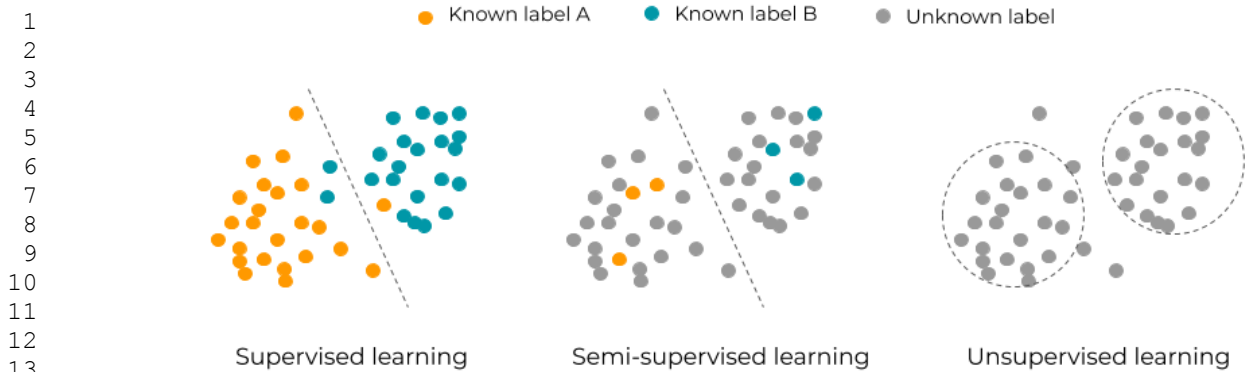
215
216 On top of these three basic learning frameworks (*supervised, unsupervised and reinforcement*
217 *learning*), there are other strategies that enable us to reuse previously trained models (*transfer*
218 *learning*) or combine models (*ensemble learning*). Transfer learning [56,57] reuses blocks and
219 layers from a model that was pre-trained with some data and for a certain task (*source domain*

220 *and task*) and fine-tune it to be applied to different data and/or task (*target domain and task*).
1 221 For example, a classification model pre-trained on ImageNet (a big collection of natural
2 222 images) can be partly reused and fine-tuned for medical imaging applications, such as organ
3 223 segmentation or treatment outcome prediction [58–60]. Transfer learning allows us to exploit
4 224 knowledge from different but related domains, mitigating the necessity of a big dataset for the
5 225 target task, and improving the model performance [60–62]. Ensemble learning methods are
6 226 also a way to improve the overall performance and the stability of the model, by combining the
7 227 output of multiple models or algorithms to perform a task [63]. Some examples of medical
8 228 applications include the mapping of patient anatomy to dose distribution for radiotherapy
9 229 treatments [64], image segmentation [65], or classification [66].
10 230

11 231 Last but not least, *self-supervised learning* is a recent **hybrid** framework that has become
12 232 state-of-the-art in natural language processing [67–69]. It is gaining attention for computer
13 233 vision tasks [70–73] and it could play an important role in future research directions for medical
14 234 imaging applications. Self-supervised learning can be seen as a variant of unsupervised
15 235 learning, in the sense that it works with unlabelled data. However, the trick here is to exploit
16 236 labels that come for “free” with the data, namely, those that can be extracted from the structure
17 237 of data itself. Self-supervised algorithms work in two steps. First, the model is pre-trained to
18 238 solve a “pretext task” where the aim is to obtain those supervisory signals from the data.
19 239 Second, the acquired knowledge is transferred and the model is fine tuned to solve the main
20 240 or “downstream task”. The literature on self-supervision for medical imaging applications is
21 241 still scarce [74–77], but for instance, a recent work used context restoration as a pretext task
22 242 [76]. Specifically, small patches in the image were randomly selected and swapped to obtain
23 243 a new image with altered spatial information, and the pretext task consisted in predicting or
24 244 restoring the original version of the image. They later used this knowledge to tune the model
25 245 for image classification of 2D fetal ultrasound images; organ localization on abdominal CT
26 246 images, and segmentation on brain MR images.
27 247

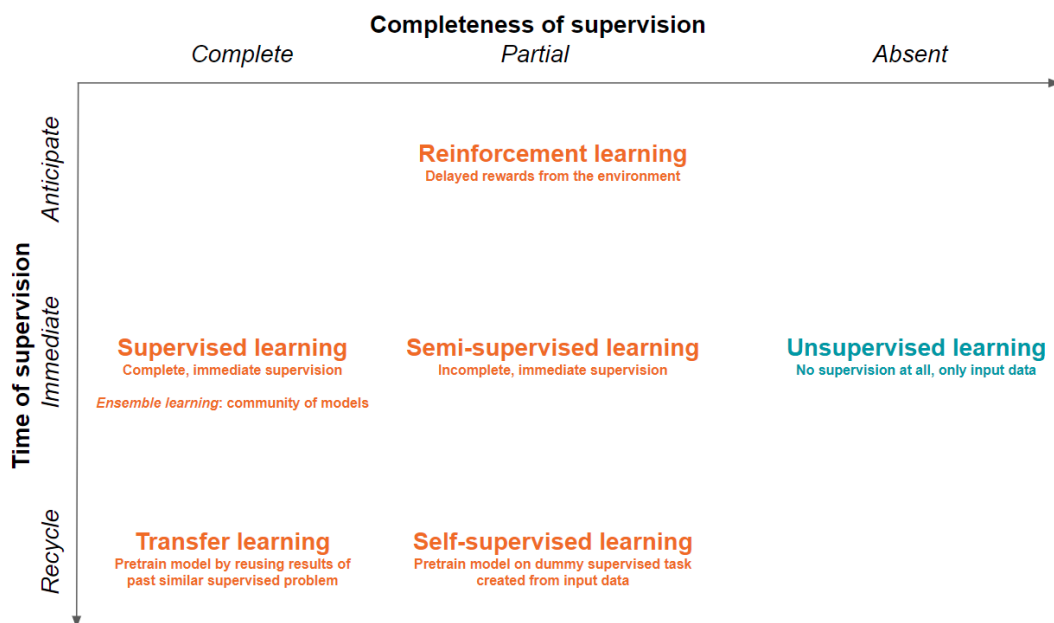
28 248 **The existence of several hybrid learning frameworks shows that the boundaries between**
29 249 **supervised and unsupervised learning has been progressively blurred to accommodate hybrid**
30 250 **framework and combined strategies (Table 1), which can address real-world problems and**
31 251 **data sets pragmatically (see Figure 3).**
32 252

33 253
34 254
35 255
36
37
38
39
40
41
42
43
44
45
46
47
48
49
50
51
52
53
54
55
56
57
58
59
60
61
62
63
64
65



1
2
3
4
5
6
7
8
9
10
11
12
13
14 256
15 257
16 258
17 259
18 260
19 261
20 262
21 263
22
23

Figure 2. Three classical learning frameworks in artificial intelligence: supervised, semi-supervised, and unsupervised learning. Supervised learning relies on known input-output pairs. If some output labels are difficult or expensive to get, semi-supervised learning can apply. If no labels are available, unsupervised learning allows for a more exploratory approach of data.



24
25
26
27
28
29
30
31
32
33
34
35
36
37
38
39
40
41
42
43
44
45 264
46 265
47 266
48 267
49 268
50 269
51 270
52 271
53 272
54 273
55 274
56 275
57 276
58
59
60
61
62
63
64
65

Figure 3. The tight framework of supervised learning can be hybridized with unsupervised learning to make room for practical cases and problems, as well as to accommodate temporality. Delaying supervision in future times leads towards reinforcement learning. Incompletely labelled data fosters semi-supervised learning, whereas small data sets encourage reusing (parts of) models trained previously on similar but bigger data sets, like in transfer learning. In self-supervision, pretraining relies on solving dummy supervised problems, where fake labels are created based on the inherent structure of image or sound data.

Learning style	Common algorithms / methods	Examples
BASIC LEARNING FRAMEWORKS		
Supervised learning	<ul style="list-style-type: none"> Linear or logistic regression Decision trees and random forests Support vector machines Convolutional neural networks Recurrent neural networks 	<ul style="list-style-type: none"> Cancer diagnosis [78–81] Organ segmentation [26,82–86] Radiotherapy dose denoising [33] Radiotherapy dose prediction [87,88] Conversion between image modalities [89,90]
Unsupervised learning	<ul style="list-style-type: none"> (Variational) Auto encoders Dimensionality reduction (e.g., Principal component analysis) Clustering (e.g., K-means) 	<ul style="list-style-type: none"> Domain adaptation tasks[35–37,91,92] Classification of patient groups [93] Image reconstruction [94]
Reinforcement learning	<ul style="list-style-type: none"> Q-learning Markov Decision Processes 	<ul style="list-style-type: none"> Tumor segmentation [54,55] Image reconstruction [95] Treatment planning [50–53,96]
HYBRID LEARNING FRAMEWORKS		
Semi-supervised learning	<ul style="list-style-type: none"> Generative Adversarial Networks 	<ul style="list-style-type: none"> Tumor classification [45,46] Organ segmentation [46] Synthetic image generation [97,98]
Self-supervised learning	<ul style="list-style-type: none"> Pretext task: distortion (e.g. rotation), color- or intensity-based, patch extraction 	<ul style="list-style-type: none"> Image classification or segmentation [76]
LEARNING STRATEGIES		
Transfer learning	<ul style="list-style-type: none"> Inductive Transductive Unsupervised 	<ul style="list-style-type: none"> Radiotherapy toxicity prediction [58] Adaptation to different clinical practices [62] Improving model generalization[99]
Ensemble learning	<ul style="list-style-type: none"> Bagging - Bootstrap AGGregatING - (e.g. random forests) Boosting (e.g. AdaBoost, gradient boosting) 	<ul style="list-style-type: none"> Radiotherapy dose prediction [100,101] Estimation of uncertainty [102] Stratification of patients[103]

Table 1. Different learning frameworks and strategies, together with some of the most popular algorithms or techniques that are used for each of them, as well as a few examples of common applications in the field of medical imaging. The table is divided in three parts: the basic learning frameworks (supervised, unsupervised and reinforcement learning), the hybrid learning frameworks blending supervised and unsupervised, and finally common learning strategies that solve consecutive learning problems or combine several models together.

2.3. Typical AI-based medical imaging analysis workflow

Reviewing past works in the AI and ML literature shows that common blocks are used in most workflows for medical imaging processing (Figure 4). As ML is driven by data, preliminary steps are to extract and select relevant features from data, that is, quantitative characteristics that summarize information conveyed by data into vectors or arrays. Then, this information is fed to generic predictive models, like classifiers or regressors, which learn to perform a certain task. An example of this strategy is the field of radiomics [104,105], where “-omics-like” features are extracted from radiological images in order to predict some indicator of interest like a disease grade or a patient's survival.

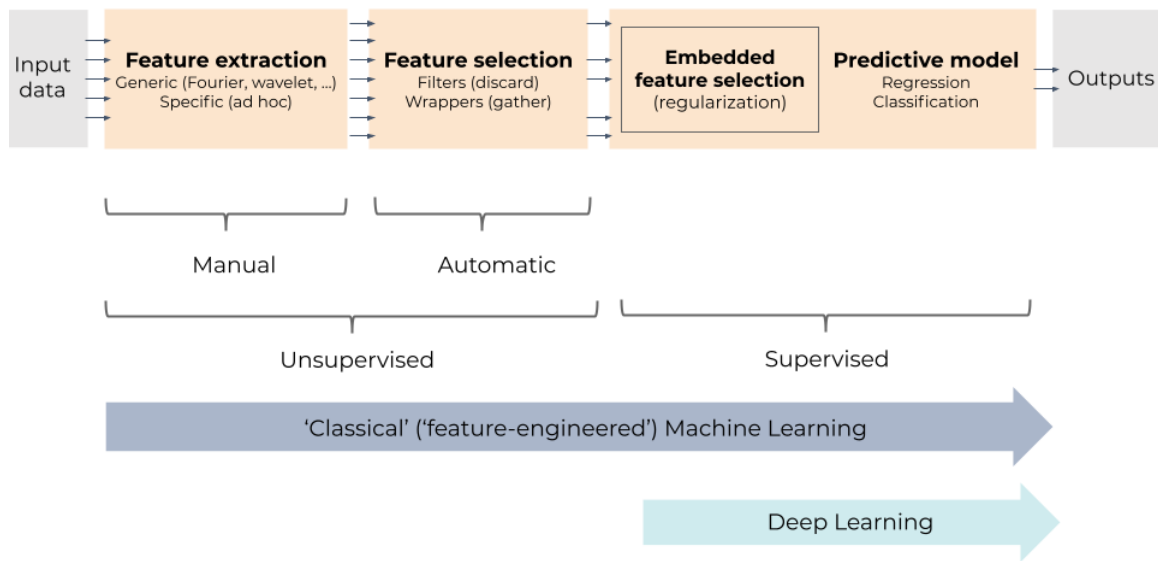


Figure 4. General ML pipeline for supervised learning: supervised predictive models are fed with features that are extracted and/or selected beforehand in an unsupervised way. Feature selection can, however, be embedded in some models, using regularization, for instance; selection then becomes supervised and therefore often improved. Classical (shallow) models tend to critically depend on unsupervised feature extraction and selection to preprocess data. In contrast, deep learning drops unsupervised feature extraction and selection; instead, it embeds multiple trainable layers of feature extractors and selectors, allowing the full pipeline to be supervised, end to end.

Feature engineering, extraction, and selection

Feature engineering, extraction, and selection are key steps to channel data to an AI method [8]. Feature engineering refers to crafting features by hand, either in ad hoc fashion or by relying on generic features from the literature. For images, the former could be gray level, color statistics, or shape descriptors (volume, diameter, curvature, sphericity, ...). Image features are often classified in local or low-level features (specific to a small group of pixels in the image) and global or high-level features (characterizing the full image). For the latter, generic features would for instance result from applying Gabor or Laplace filters, edge detectors like Sobel operators, texture descriptors, Zernike moments, or popular transforms like Fourier's or wavelet bases. In radiomics, all the above mentioned features can be used

317 together, like ad hoc tumor shape and intensity descriptors, as well as textural descriptors
1 318 (typically, Haralick's gray level co-occurrence matrix [106]).

2 319
3
4 320 As an alternative or in a second time, higher-level features can be extracted in a more data-
5 321 driven way, using dimensionality reduction. Methods like Principal Component Analysis [107],
6 322 Linear Discriminant Analysis [108], auto-associative [109] networks can reduce the number of
7
8 323 input variables according to some unsupervised or supervised criterion. For images more
9 324 specifically, the convolutional filters involved in CNNs bear similarity with the filters above: they
10 325 extract local features, but their parameters are learnt from data and stacking them allows the
11 326 global higher-level features to emerge. When features are not extracted in a supervised, data-
12 327 driven way, it might happen that some of them are redundant or not relevant. To address this
13
14 328 issue, a feature selection step can discard those to focus on a reduced set of features. Feature
15 329 selection can follow several strategies, by either selecting or discarding. Wrappers [110] use
16 330 a supervised predictive model to score subsets of features. To avoid the burden of a full
17 331 fledged predictive model, feature filters [111], not to be confused with image filters above, use
18 332 an unsupervised surrogate to score feature subsets, like their correlation or mutual
19 333 information. Embedded methods [112] are directly integrated into the predictive model. For
20 334 instance, feature weight regularization can favor sparse configurations, where irrelevant
21 335 features get null weights. Examples of features selection in radiomics can be found in [113–
22 336 119], for instance. Deep neural networks typically rely on this last approach with regularization.
23 337 In the example of radiomics, embedded feature selection can be implemented with deep
24 338 neural networks [120] and regularization, hence allowing for end-to-end learning instead of
25 339 combining manually engineered features with shallow predictive models.

30 340 31 341 ***Predictive models***

32 342
33 343 Common tasks in AI are regression and classification. The AI/ML model then attempts to
34 344 predict either continuous values (e.g., a dose or a survival time) or class probabilities (e.g.,
35 345 benign vs malignant) starting from input features. In the following, we describe the main
36 346 methodological aspects of the basic predictive ML models, state-of-the-art ML/DL methods
37 347 and examples of their clinical applications for medical imaging are presented in the next
38 348 section.

39 349
40
41 350 Regression is the most generic task in supervised learning. Linear regression is well known
42 351 but other mathematical models can involve exponential or polynomial functions. ML
43 352 generalizes this concept to universal approximators that can fit data sampled from almost any
44 353 smooth function, with also possibly many input and output variables. Artificial neural networks
45 354 (NNs) are the most iconic universal approximators (Figure 5). They consist of interconnected
46 355 formal models of neurons, a mathematical 'cell' combining several 'dendritic' inputs into a
47 356 weighted sum that triggers an 'axonal' output through a nonlinear activation function, like a
48 357 step, a sigmoid, or a hinge (Rectified Linear Unit, ReLU).

49 358 As soon as a hidden layer of neurons with nonlinear activation functions is inserted between
50 359 the input and the output layers, a NN becomes a universal approximator [121]. However, a
51 360 notion of capacity is associated with the NN architecture: the more neurons the hidden layer
52 361 counts, the more complex functions can be approximated. The capacity is roughly proportional
53 362 to the number of synaptic weights (parameters) in the NN and it is analogous to the polynomial
54 363 order in polynomial regression (the number of weights in the terms). Deep NNs are obviously
55 364 also universal approximators [121,122]. Their interest lies in trading width of a single hidden
56 365

365 layer for depth, as stacks of hidden layers allow functional difference (e.g., convolutive
1 366 neurons for image data) and thus hierarchical processing, explaining the later success of deep
2 367 networks compared to shallow ones. Most NNs are feed-forward, meaning that data flows
3 368 unidirectionally from inputs to outputs. Recurrent NNs (RNNs) add feedback loops to
4 369 feedforward connections, allowing them to process sequences of data (text, videos) and
5 370 somehow to keep memories of past inputs, which then gives context to new inputs.
6 371 Training of NNs relies on minimizing a loss function between the desired output and the one
7 372 provided by the NN in its current parameter configuration. The partial derivatives, or gradient,
8 373 of the loss function with respect to these parameters indicates the direction in which tuning
9 374 the parameters is likely to decrease the loss. In a feedforward NN, this derivative information
10 375 flows back from layer to layer and is therefore called gradient backpropagation.
11 376 For regression, typical loss functions can be the mean square error or mean absolute error.
12 377 With a suitable change of the output layer (softmax or normalized exponential) and loss
13 378 function (the cross entropy), the NN can approximate class probabilities.
14 379

15 380 Classification is the other prominent task in ML. Classifiers are simply algorithms that can sort
16 381 data into groups or categories, and there exists a large variety of them [123]. Some of the
17 382 most popular ones are very intuitive and easy to interpret, such as decision trees [124], where
18 383 input data is classified [by going through a hierarchical, tree-like process including different](#)
19 384 [branching tests of the data features \(Figure 6.a\). Growing several complementary decision](#)
20 385 [trees together, in an ensemble learning strategy, leads to random forests \(Figure 6.b, see also](#)
21 386 [Section 3\)](#). Other simple algorithms for classification include the linear classifier, the Bayesian
22 387 classifier, or the Perceptron (Figure 5.a). More sophisticated algorithms can actually be used
23 388 for both regression and classification tasks. Some examples are NNs (Figure 5.b), which can
24 389 yield class probabilities with suitable output layers; or support vector machines [125], which
25 390 can be seen as an improved linear classifier that works in a higher-dimensional space and try
26 391 to fit the separation (hyper)plane with the thickest margin in between points of two classes
27 392 (Figure 7).
28 393
29 394
30 395
31 396
32 397
33 398
34 399
35 400
36 401
37 402
38 403
39 404
40 405
41 406
42
43
44
45
46
47
48
49
50
51
52
53
54
55
56
57
58
59
60
61
62
63
64
65

1
2
3
4
5
6
7
8
9
10
11
12
13
14
15
16
17
18
19
20
21
22
23
24
25
26
27
28
29
30
31
32
33
34
35
36
37
38
39
40
41
42
43
44
45
46
47
48
49
50
51
52
53
54
55
56
57
58
59
60
61
62
63
64
65

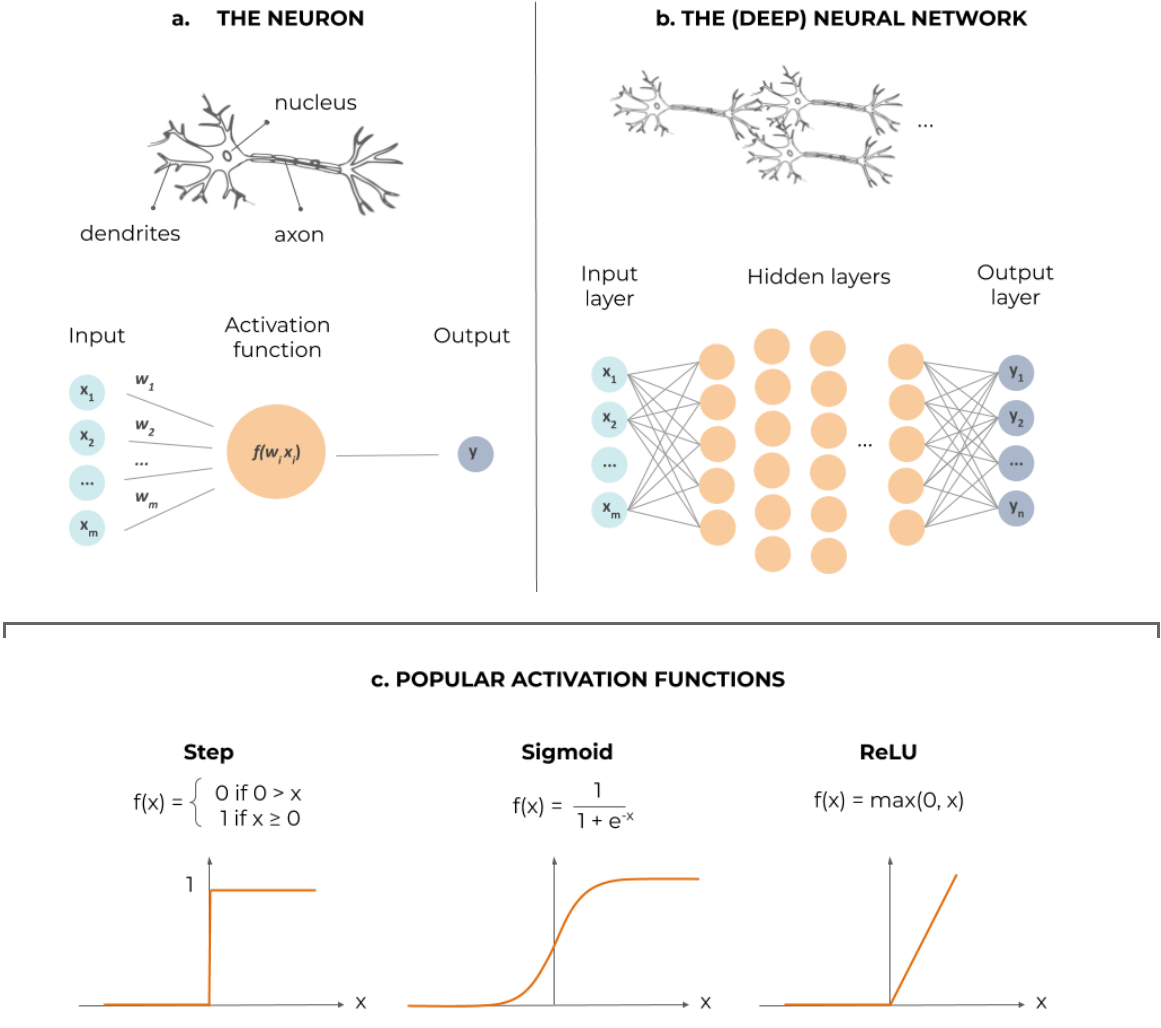


Figure 5. Artificial neural networks in a nutshell. (a) The formal neuron, processing several dendritic inputs through a nonlinear activation function f , to produce its actional output. (b) The neurons can be interconnected in a feed-forward way, into successive layers; as soon as a nonlinear 'hidden' layer is inserted in between the inputs and outputs, the network can potentially approximate any function; specific activation functions can be fitted in the output layer to achieve either regression or classification. (c) Examples of nonlinear activation functions in the hidden layers: the step function, from biological inspiration, the sigmoid, its continuous and differentiable surrogate, and the rectified linear unit (ReLU), that improves training of deep layers.

407
408
409
410
411

1
2
3
4
5
6
7
8
9
10
11
12
13
14
15
16
17
18
19
20
21
22
23
24
25
26
27
28
29
30
31
32
33
34
35
36
37
38
39
40
41
42
43
44
45
46
47
48
49
50
51
52
53
54
55
56
57
58
59
60
61
62
63
64
65

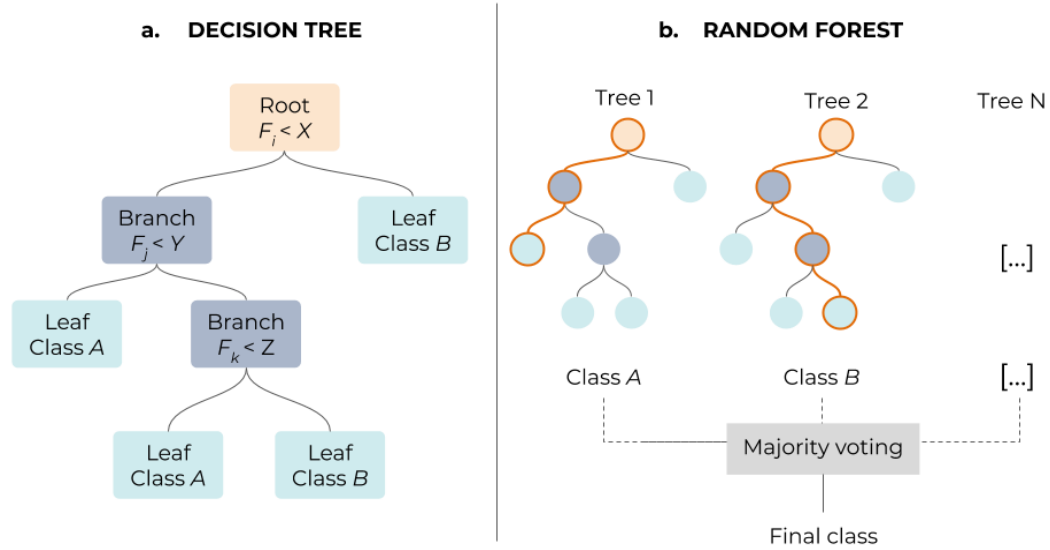
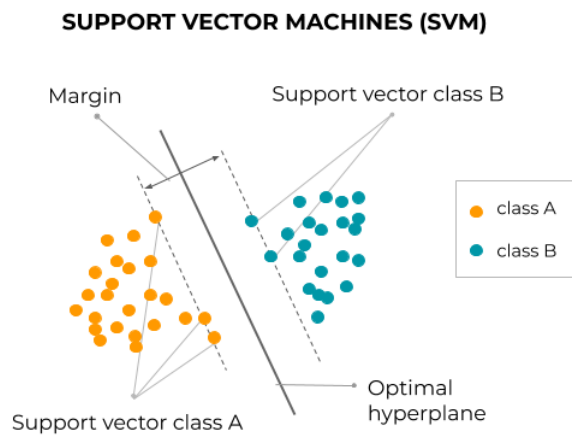


Figure 6. (a) Decision trees assign labels (*leafs*) to a given sample by going through a multi-level structure where different features (*root nodes*) and solutions (*branches*) are tested. (b) In a Random Forest algorithm, decision trees are combined, following an ensemble learning approach, which enables to get more accurate predictions than a single tree. Each individual tree in the forest spits out a class prediction and the class with the most votes becomes the final model's prediction.

412
413



414
415
416
417
418
419
420
421
422
423

Figure 7. Principle of the linear support vector machine, which lifts the indeterminacy of separable classification by fitting the thickest margin, stuck in between a few 'support vectors'. The principle can be extended to nonlinear class separation by using Mercer kernels [125].

3. State-of-the-art AI methods for medical image analysis

In the last decade, intensive research in AI methods for medical applications, and specifically in ML/DL (Figure 8, left), yielded thousands of publications reporting the performance of new algorithms and/or original variants of the existing ones. The number of publications using some of the most popular ML/DL methods is presented in Figure 8. In particular, in recent years, attention has moved from ML methods such as SVMs and Random Forests to Convolutional Neural Networks (Figure 8, right). In addition, since 2018, the use of other DL methods such as Generative Adversarial Networks or reinforcement learning algorithms is rapidly increasing. Notice that this section is not intended to be an exhaustive review of the application of AI methods to the medical field, but rather an illustration of the potential of these methods. Thus, in the following, we describe the basic methodological aspects of two of the most widely used algorithms (Random Forests and CNNs), as well as the increasingly popular GANs, and we provide some examples of recent applications of these methods to the field of medical image processing.

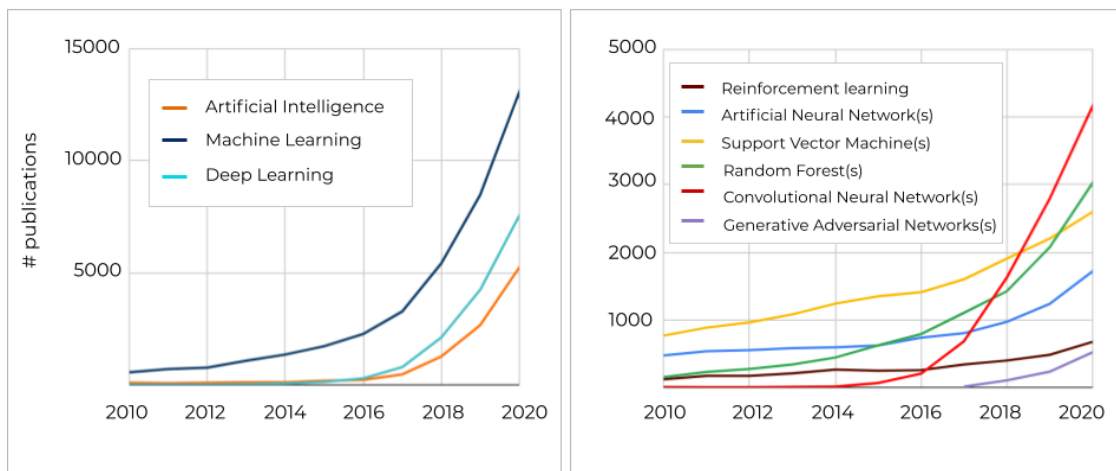


Figure 8. Number of publications since 2010 till 2020 in the PubMed repository, containing keywords related to AI/ML/DL methods in the title and/or abstract.

Random Forests (RFs)

Random forests (RFs) [126,127] use an ensemble of uncorrelated binary decision trees (multiple learning models) to find the best predictive model (Figure 6). Each decision tree can be seen as a base model (binary classifier) with its respective decision, where a combination of such decisions leads to the final output. This is achieved in RFs by using two distinctive mechanisms, i.e., internal feature selection and voting [128]. The RFs algorithm extracts a multitude of low-level (simple) data representations and uses the feature selection mechanism on all collected features to find the most informative ones. After feature selection, a majority vote on selected classifiers yields the final decision. For a full detailed description of the RF algorithm we refer to [128].

The earliest applications of RFs date from a decade ago for organ localization [129] and delineation [130]. Since then, RFs have been applied to numerous tasks, including detection and localization, segmentation, and image-based prediction [128]. For some specific

459 applications, RFs have demonstrated an improved performance over other classical ML
1 460 methods. For instance, Deist et al. [131,132] compared six different classification algorithms
2 461 (decision tree, RFs, NNs, SVM, elastic net logistic regression, LogitBoost) on 12 datasets with
3 462 a total of 3496 patients, for outcome and toxicity prediction in (chemo)radiotherapy. They
4 463 concluded that RFs was the algorithm achieving higher discriminative performance (on 6 over
5 464 12 datasets). This goes in line with the findings from more fundamental ML research studies,
6 465 which have reported RFs as one of the best classical learning algorithms [133]. However,
7 466 many other works in the medical field have also compared the accuracy of RFs against more
8 467 complex or simpler ML classifiers, and it is well known that their performance may vary for
9 468 different applications [103,113,132,134–139] and even for different datasets within the same
10 469 application [131,132]. This makes it hard to conclude on the absolute superiority of RFs
11 470 algorithm over other ML classifiers. Nevertheless, the work of Deist et al. included one of the
12 471 largest datasets investigated so far for radiotherapy outcome prediction, which is a strong
13 472 argument in favor of considering RFs as one of the first options to investigate for this kind of
14 473 application. In addition, RFs keep achieving very promising results in recent applications
15 474 related to outcome prediction [135,139–143], but also for other domains like image
16 475 classification [113,144] or automatic treatment planning [100,145–147]. Regarding other tasks
17 476 where RFs were among the state-of-the-art methods a few years ago, like image synthesis
18 477 [148–150] or segmentation [151,152], the community has now fully switched the attention to
19 478 CNNs [5,153,154]. Nevertheless, in favor of RFs one could argue that they are easy to
20 479 implement and less computationally expensive than CNNs (i.e., they can work in regular CPU).
21 480 Therefore, they still deserve an important place in the ML toolbox for medical imaging.
22 481

29 482 *Convolutional Neural Networks (CNNs)*

30 483
31 484 Convolutional neural networks (CNNs) are inspired by the human visual system and exploit
32 485 the spatial arrangement of data within images. Their remarkable capacity to detect hierarchical
33 486 data representations has made CNNs the most popular architecture for current medical image
34 487 processing applications.
35 488

36 489 Traditionally, CNNs stack successive layers of convolutions and down-sampling, and fully
37 490 connected layers towards the output (Figure 9). Sequential applications of multiple
38 491 convolutions enable the network to extract first simple features, like edges, in the deepest
39 492 layers, which are next combined and refined into richer, more complex, hierarchical features,
40 493 like full organs. Within each convolutional layer, feature saliency is determined by scanning a
41 494 fixed-size convolution kernel (typically 3x3) all over the image to yield a feature map. This
42 495 allows for an economy of parameters (weight sharing) and hence easier training.
43 496 Downsampling layers are inserted between convolutional layers to reduce the size of feature
44 497 maps, typically by applying a max-pooling operation, which keeps the maximum pixel value
45 498 out of all non-overlapping 2-by-2 blocks in the feature map. To some extent, successive max-
46 499 pooling allows for some shift invariance with respect to image content, as the salient maximum
47 500 might stem from anywhere in the block. Downsampling trades resolution for number, as more
48 501 convolution filters can be applied to smaller features maps within the same memory footprint.
49 502 Eventually, fully connected layers generate the outputs, where all neurons are inter-
50 503 connected.
51 504

52 505 Fully convolutional networks (FCNs) [155] were proposed to efficiently perform image-to-
53 506 image tasks like segmentation. In CNNs, repeated convolution and max-pooling layers lead
54
55
56
57
58
59
60
61
62
63
64
65

507 to low resolution abstract outputs. In order to return to full-resolution images, fully connected
1 508 layers in CNNs are replaced in FCNs with operations that revert convolution and max-pooling.
2 509 Following the same line, U-net [156] was presented for biomedical image segmentation, and
3 510 is now widely used in medical imaging. It is an encoder-decoder styled network, where the
4 511 encoder can be seen as a feature extraction block, and the decoder as output generation
5 512 block. Within medical imaging, FCNs are used in both supervised, and unsupervised settings
6 513 depending on the respective architecture. In supervised training, FCNs are mostly used for
7 514 discriminative tasks, such as detection, localization, classification, segmentation, and
8 515 denoising. Note that CNNs and FCNs are often used interchangeably.
9 516

10 517 For certain applications, such as image segmentation [154,157,158] or synthesis [5], CNNs
11 518 are now considered the state-of-the-art methods [4]. Although the comparison of different
12 519 algorithms on the same dataset is not so common, an excellent way to track the evolution of
13 520 the state-of-the-art algorithms is to look at the challenges and competitions organised around
14 521 specific topics. In certain cases, CNNs have clearly surpassed the performance of more
15 522 classical methods. A good example is the Challenge on Liver Ultrasound Tracking (CLUST):
16 523 the winning team in the first edition (2014) achieved a tracking error of 1.51 ± 1.88 mm using
17 524 an approach based on image registration algorithms [159]; whereas the current best
18 525 performing algorithm, based on CNNs, achieves under 1 mm accuracy (0.69 ± 0.67 mm),
19 526 demonstrating a more robust model [160]. Another example is the database from the MICCAI
20 527 Head and Neck Auto-segmentation Challenge 2015 [161], for which the most recent methods
21 528 based on CNNs [26,162–164] has improved the Dice coefficients obtained at that time with
22 529 model- and atlas-based algorithms by more than 3% on average. In particular, the work of
23 530 Nikolov et al [26] has recently reported a U-Net architecture with an accuracy equivalent to
24 531 experienced radiographers. These are just two of the many competitions organised around
25 532 medical imaging tasks [165], but year after year CNNs are becoming the backbone of the best
26 533 performing algorithms.
27 534

28 535 Some of the latest methodological improvements in the architecture of CNNs that have
29 536 contributed to more robust and accurate models include coarse-to-fine cascade of two CNNs
30 537 [166] to address class-imbalance issues; the addition of squeeze-and-excitation (SE)-blocks
31 538 to allow the network to model the channel and spatial information separately [167], increasing
32 539 the model capacity; or the implementation of attention mechanisms, which enables the
33 540 network to focus only on most relevant features [168–170].
34 541

35 542 Besides image segmentation, other recent successful applications of CNNs include
36 543 classification [171,172], outcome prediction [120,173,174], automatic treatment planning
37 544 [62,87,175], motion tracking [176,177] or image enhancement [33]. In numerous applications,
38 545 CNNs have either demonstrated an accuracy similar to human experts [26,80,178,179],
39 546 decreased the interobserver variability [180,181] or reduced the physician's workload for a
40 547 specific task [157]
41
42
43
44
45
46
47
48
49
50
51
52
53
54
55
56
57
58
59
60
61
62
63
64
65

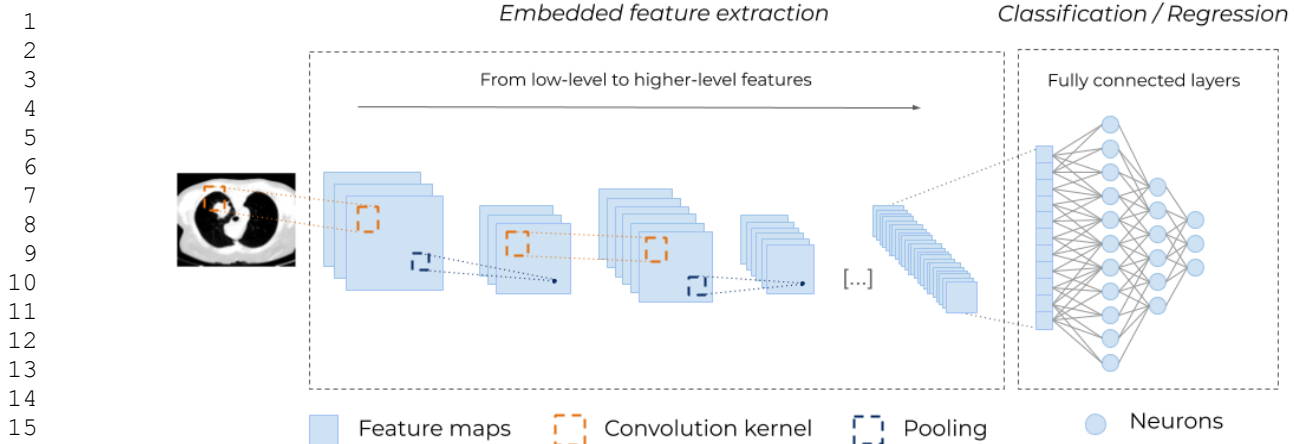


Figure 9. Typical architecture for a (deep) Convolutional Neural Network (CNN). Different convolutional kernels scan the input images leading to several feature maps. Then, down-sampling operations, such as max-pooling (i.e., taking the maximum value of a block of pixels), are applied to reduce the size of the feature maps. These two operations, convolution and pooling, are applied multiple times to extract higher-level features. At the end, the feature maps are flattened and passed through fully connected layers of neurons (see Figure 5), to obtain a final prediction. The embedded (automatic and unsupervised) feature extraction (Figure 4) is what enables CNNs to remove all hand-crafted operations and makes them so powerful.

548

549 *Generative adversarial networks (GANs)*

550

551 Generative adversarial networks (GANs) [182] are popular architectures used for generative
 552 modeling. GANs consists of two networks: generator \mathcal{G} and discriminator \mathcal{D} (Figure 10). The
 553 intuition is that \mathcal{G} iteratively tries to map a random input distribution to a given data distribution
 554 to generate new data, which \mathcal{D} evaluates. Depending on the feedback from \mathcal{D} , \mathcal{G} tends to
 555 minimize the loss between the two distributions, thus generating similar samples as input data.
 556 The goal is to trick \mathcal{D} into classifying generated data as real. Both networks are trained
 557 simultaneously to get better at their respective tasks: while \mathcal{G} is learning to fool \mathcal{D} , \mathcal{D} is
 558 concurrently learning to better distinguish generated data from real input data. Note that both
 559 \mathcal{D} and \mathcal{G} are generally CNNs trained in an adversarial setup.

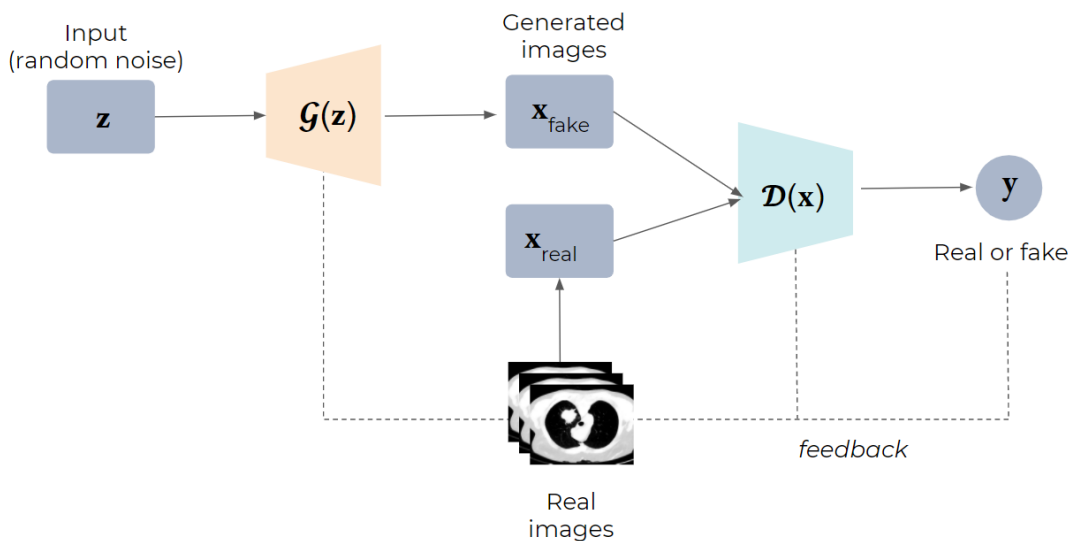
560

561 Unlike CNNs, which have relatively old foundations dating back to 1980 (Section 2),
 562 adversarial learning is a rather new concept. However, it has rapidly rooted in the medical
 563 imaging field, leading to numerous publications in the last few years [183,184]. The initially
 564 proposed architecture for GANs [182] suffered from several drawbacks, such as a very
 565 unstable training, but the intensive research in the field of computer vision has lead substantial
 566 improvements by either changing the architecture of \mathcal{D} and \mathcal{G} , or investigating new loss
 567 functions [183,185]. A way to better control the data generation process in GANs is to provide
 568 extra information about the desired properties of the output (e.g. examples of the desired real
 569 images or labels). This is known as conditional GANs (cGANs) [186], and it can be categorized
 570 as a form of supervised learning since it requires aligned training pairs. However, we believe
 571 that the real strength of GANs relies on their ability to learn in a semi-supervised or fully
 572 unsupervised manner. Specifically, in the medical imaging field, where aligned and properly

573 annotated image pairs are seldom available, GANs are starting to play a very important role.
1 574 In this context, cycleGANs [187] is probably one of the most famous architectures allowing
2 575 bidirectional mapping between two domains using unpaired input data.
3 576

5 577 So far, in the medical imaging field, GANs have been mostly applied to synthetic image
6 578 generation for data augmentation [188–190] and multi-modality image translation (e.g. MR to
7 579 CT [90,191–193], CBCT to CT [97,194], among others [5,183]). Regarding data augmentation
8 580 applications, we believe that GAN-based models have the potential to better sample the whole
9 581 data distribution and generate more realistic images than traditional approaches (e.g. rotation,
10 582 flipping, etc), which may contribute to a higher generalizability of the model [188] and more
11 583 efficient training [195]. For multi-modality image translation, although cGANs have achieved
12 584 good results [90,191,193,196], cycleGANs usually outperforms in terms of accuracy, in
13 585 addition to overcome the issues related to paired image training (i.e. inaccurate aligning or
14 586 labelling) [39,97,194,197]. Besides image translation, GANs have also been applied to other
15 587 tasks, such as segmentation [198–203] or radiotherapy dose prediction [204–207], or artifact
16 588 reduction [208], among others [183].
17 589

20 590 All above-mentioned applications have explored the generative capacity of GANs, but we
21 591 believe that their discriminate capacity may also have some potential, since it can be used as
22 592 regularized or detector when provided with abnormal images [209], which might be an
23 593 excellent application for quality assurance tasks in radiation oncology, for instance.
24 594
25 595



596
597
598 Figure 10. Structure of Generative Adversarial Networks (GANs). Starting from random noise, the
599 generator (G) uses the feedback from the discriminator (D) and learns to create images that are similar
600 to the provided ground truth.
601
602
603
604
605
606

4. Discussion and concluding remarks: where do we go next?

This article provided an overview of AI with a focus on medical imaging analysis, paying attention to key methodological concepts and highlighting the potential of the state-of-the-art ML and DL methods to automate and improve different steps of the clinical practice. Incorporating such knowledge into the clinical practice and making it accessible to the medical community will definitely help to demystify this technology, inspire new and high quality research directions, and facilitate the adoption of AI methods in the clinical environment.

Looking at the evolution of AI methods, one can certainly conclude that shifting from computationalism to connectionism, together with the transition from shallow to deep architectures, has brought a disruptive transformation to the medical field. However, an important part of the research so far has focused on simply translating the latest ML/DL advances in the field of computer vision to medical applications, in order to demonstrate the potential of these methods and the feasibility to use them to improve the clinical practice. It is the case of some of the papers cited in this manuscript, such as the first proof-of-concepts of the use of CNNs for organ segmentation [32] and for dose prediction for radiotherapy treatments [34], or the use of GANs for conversion between image modalities [97]. Although the technological transfer from computer science to the medical field will certainly continue to bring important progress, the next generation of AI methods for medical applications will only emerge if the medical community steps up to embrace AI technology and integrate all the domain-specific knowledge into the state-of-the-art AI methods [210,211]. This can be done in several ways, such as adding extra information in the input channels of the models or using dedicated loss functions during the model training. Some groups have already started to explore these research directions. For instance, instead of using generic loss functions from computer vision tasks, like the mean squared error, one could use loss functions that better target the specificities of our medical problem, such as including mutual information for the conversion of different image modalities [90,193] or dose-volume histograms for radiotherapy dose predictions [212]. Regarding the injection of domain-specific knowledge as input to the models, some examples include the addition of electronic health records and clinical data, like text and laboratory results, to the image data [213–215], or having first-order prior or approximations of the expected output [175,216–219]

Integrating domain-specific knowledge cannot only serve to improve the performances of state-of-the-art AI models, but also to increase the interpretability of the results, which is one of the well-acknowledged limitations of the current ML/DL methods [220–223]. This is the idea behind the so-called Expert Augmented Machine Learning (EAML), whose goal is to develop algorithms capable of extracting human knowledge from a panel of experts and use it to establish constraints for the model's prediction [224]. This "human-in-the-loop" approach is also useful to train our AI models more efficiently. Indeed, some preliminary studies have reported that blindly increasing the training databases will not bring much improvement to our AI model's performance [225]. In contrast, active learning [226] is a type of iterative supervised learning that follows this human-in-the-loop concept, where the algorithm itself query the user to obtain new data points where they are most needed, in order to build up an optimally balanced training dataset [227,228]. Nevertheless, although a human-centered approach for AI models is certainly the way to go in the close future, parallel research should focus on implementing strategies that leverage the problem of data labelling with semi-supervised, unsupervised or yet the increasingly popular self-supervised learning.

The quality of the data itself is certainly another important aspect that is worth discussion. Data collection and curation are indeed of paramount importance, since errors, biases, or variability in the training databases are often directly reflected in the model behavior and can have dramatic consequences in the model performances and its clinical outcome. Some examples of these issues include gender imbalance [229], racial bias [230], or data heterogeneity due to changes in treatment protocols over time [225]. Despite progress in AI methods, data collection remains poorly automatized

659 and the time dedicated to data collection and curation is often overly long. In fact, most state-of-the-art
1 660 AI algorithms can be trained in a few hours, whereas building a large-scale well curated database can
2 661 take months. Therefore, the same way physicians are familiar with planning protocols or delineation
3 662 guidelines, the clinical teams should start being familiar with guiding principles for data management
4 663 and curation in the era of AI. The FAIR (Findability, Accessibility, Interoperability, and Reusability) Data
5 664 Principles [231] are the most popular and general ones, but the medical community should focus efforts
6 665 on adapting those principles to the specificities of the medical domain [232–234]. Only in this way, we
7 666 will manage to have a safe and efficient clinical implementation of AI methods. In addition, federated
8 667 learning approaches [235–237] can be used to train AI models across institutions while ensuring data
9 668 privacy protection, sharing the clinical knowledge and getting the advantages of collaborative AI
10 669 solutions.

11 670
12 671 Investing time and collaborative effort in high-quality databases is certainly the way to move forward.
13 672 So far, two aspects have played an important role in the recent development of AI and ML, namely,
14 673 data repositories [238] and contests [239,240], the former feeding the latter. Competitions generate
15 674 emulation among actors of the domain and allow state-of-the-art models to be benchmarked. A few
16 675 examples have been cited in this manuscript, but there are multiple competitions every year that lead
17 676 to public data repositories [241–243]. A very recent example is the breakthrough of AI in the CASP
18 677 competition [244]. However, the results and rankings from competitions must be interpreted carefully
19 678 when transferring the acquired knowledge into clinical applications [245,246]. Due to the high stakes in
20 679 the medical domain, the community should devote even stronger efforts and international organizations
21 680 should emit recommendations for data collection and curation, as well as for the design of contests and
22 681 competitions. In the long term, this would lead to a much more structured and uniform clinical practice,
23 682 with reduced differences between centres. Bigger, more homogeneous data could then potentially allow
24 683 for another level of AI, by extracting much finer information, at the level of large populations. If data for
25 684 AI is still in its infancy, so are also the methods. In spite of amazing progress and wowing results, current
26 685 AI remains cast within tight frameworks. AI for images has been dealt here. Other application domains
27 686 focus on natural language and speech processing with related but quite different approaches. So far,
28 687 computer vision and audition follow different specialized approaches, although some works attempt to
29 688 bridge the gap, like automatic image captioning. Nevertheless, these blocks remain mostly separated
30 689 and current AI blocks lack integration and are still considered as weak AI. For instance, typical CNNs
31 690 can boil down to just big filter banks, without any notion of time, and thus no memory and no experience.
32 691 Strong AI is going to emerge when AI for images and speech, as well as active learning [227,228], will
33 692 be combined into a sort of Frankensteinian brain, in which specialized lobes for the different senses get
34 693 interconnected. This will allow for richer interaction, explainability through speech, reference to past
35 694 experience, and continuous improvement. Such a strategy has been paved for autonomous driving,
36 695 with different levels of automation. Confidence into ever more complex AI will grow only if AI can get
37 696 more anthropomorphic, at least from a functional point of view.

38 697
39 698 [In conclusion, artificial intelligence methods, and in particular, machine and deep learning methods,](#)
40 699 [have reached important milestones in the last few years, demonstrating their potential to improve and](#)
41 700 [automate the medical practice. However, a safe and full integration of these methods into the clinical](#)
42 701 [workflow still requires a multidisciplinary effort \(computer science, IT, medical experts, ...\) to enable the](#)
43 702 [next generation of strong AI methods, ensuring robust and interpretable AI-based solutions.](#)

44 703
45 704
46 705
47 706
48 707
49 708
50 709
51 710
52
53
54
55
56
57
58
59
60
61
62
63
64
65

711 **Acknowledgements**

1 712
2 713 Ana Barragán is funded by the Walloon region in Belgium (PROTHERWAL/CHARP, grant
3 714 7289). Gilmer Valdés was supported by the National Institute of Biomedical Imaging and
4 715 Bioengineering of the National Institutes of Health under Award Number K08EB026500. Dan
5 716 Nguyen is supported by the National Institutes of Health (NIH) R01CA237269 and the Cancer
6 717 Prevention & Research Institute of Texas (CPRIT) IIRA RP150485. Liesbeth Vandewinckele
7 718 is supported by a Ph.D. fellowship of the research foundation - Flanders (FWO), mandate
8 719 1SA6121N. Kevin Souris is funded by the Walloon region (MECATECH / BLOWIN, grant
9 720 8090). John A. Lee is a Senior Research Associate with the F.R.S.-FNRS.

10 721

11 722 **References**

- 12 723
13 724
14
15
16
17
18
19 725 [1] Singh R, Wu W, Wang G, Kalra MK. Artificial intelligence in image reconstruction: The
20 726 change is here. *Phys Med* 2020;79:113–25.
21 727 [2] Wang M, Zhang Q, Lam S, Cai J, Yang R. A Review on Application of Deep Learning
22 728 Algorithms in External Beam Radiotherapy Automated Treatment Planning. *Front Oncol*
23 729 2020;10:580919.
24 730 [3] Wang C, Zhu X, Hong JC, Zheng D. Artificial Intelligence in Radiotherapy Treatment
25 731 Planning: Present and Future. *Technol Cancer Res Treat* 2019;18:1533033819873922.
26 732 [4] Litjens G, Kooi T, Bejnordi BE, Setio AAA, Ciompi F, Ghafoorian M, et al. A survey on
27 733 deep learning in medical image analysis. *Medical Image Analysis* 2017;42:60–88.
28 734 <https://doi.org/10.1016/j.media.2017.07.005>.
29 735 [5] Wang T, Lei Y, Fu Y, Wynne JF, Curran WJ, Liu T, et al. A review on medical imaging
30 736 synthesis using deep learning and its clinical applications. *J Appl Clin Med Phys*
31 737 2021;22:11–36.
32 738 [6] Thompson RF, Valdes G, Fuller CD, Carpenter CM, Morin O, Aneja S, et al. Artificial
33 739 intelligence in radiation oncology: A specialty-wide disruptive transformation?
34 740 *Radiotherapy and Oncology* 2018;129:421–6.
35 741 <https://doi.org/10.1016/j.radonc.2018.05.030>.
36 742 [7] Hosny A, Parmar C, Quackenbush J, Schwartz LH, Aerts HJWL. Artificial intelligence in
37 743 radiology. *Nat Rev Cancer* 2018;18:500–10.
38 744 [8] Morra L, Delsanto S, Correale L. Artificial Intelligence in Medical Imaging 2019.
39 745 <https://doi.org/10.1201/9780367229184>.
40 746 [9] Ranschaert ER, Morozov S, Algra PR, editors. Artificial Intelligence in Medical Imaging:
41 747 Opportunities, Applications and Risks. Springer, Cham; 2019.
42 748 [10] Friedman J, Hastie T, Tibshirani R. The elements of statistical learning. vol. 1. Springer
43 749 series in statistics New York; 2001.
44 750 [11] Kuhn M, Johnson K. Applied Predictive Modeling. Springer, New York, NY; 2013.
45 751 [12] Shen C, Nguyen D, Zhou Z, Jiang SB, Dong B, Jia X. An introduction to deep learning in
46 752 medical physics: advantages, potential, and challenges. *Phys Med Biol*
47 753 2020;65:05TR01.
48 754 [13] Cui S, Tseng H, Pakela J, Ten Haken RK, El Naqa I. Introduction to machine and deep
49 755 learning for medical physicists. *Medical Physics* 2020;47.
50 756 <https://doi.org/10.1002/mp.14140>.
51 757 [14] Holman JG, Cookson MJ. Expert systems for medical applications. *J Med Eng Technol*
52 758 1987;11:151–9.
53 759 [15] Haug PJ. Uses of diagnostic expert systems in clinical care. *Proc Annu Symp Comput*
54 760 *Appl Med Care* 1993:379–83.
55 761 [16] Miller RA. Medical diagnostic decision support systems--past, present, and future: a
56 762 threaded bibliography and brief commentary. *J Am Med Inform Assoc* 1994;1:8–27.

61
62
63
64
65

- 763 [17] Buchanan BB, . Buchanan BG, Buchanan BG, Shortliffe EH, Heuristic S. Rule-based
1 764 Expert Systems: The MYCIN Experiments of the Stanford Heuristic Programming
2 765 Project. Addison Wesley Publishing Company; 1984.
- 3 766 [18] Aikins JS, Kunz JC, Shortliffe EH, Fallat RJ. PUFF: an expert system for interpretation
4 767 of pulmonary function data. *Comput Biomed Res* 1983;16:199–208.
- 5 768 [19] Miller RA, Pople HE Jr, Myers JD. Internist-1, an experimental computer-based
6 769 diagnostic consultant for general internal medicine. *N Engl J Med* 1982;307:468–76.
- 7 770 [20] Buchanan BG. Can Machine Learning Offer Anything to Expert Systems? In: Marcus S,
8 771 editor. *Knowledge Acquisition: Selected Research and Commentary: A Special Issue of*
9 772 *Machine Learning on Knowledge Acquisition*, Boston, MA: Springer US; 1990, p. 5–8.
- 10 773 [21] Su MC. Use of neural networks as medical diagnosis expert systems. *Comput Biol Med*
11 774 1994;24:419–29.
- 12 775 [22] Aizenberg IN, Aizenberg NN, Vandewalle J. Multi-Valued and Universal Binary Neurons
13 776 2000. <https://doi.org/10.1007/978-1-4757-3115-6>.
- 14 777 [23] Liu X, Faes L, Kale AU, Wagner SK, Fu DJ, Bruynseels A, et al. A comparison of deep
15 778 learning performance against health-care professionals in detecting diseases from
16 779 medical imaging: a systematic review and meta-analysis. *Lancet Digit Health*
17 780 2019;1:e271–97.
- 18 781 [24] Esteva A, Kuprel B, Novoa RA, Ko J, Swetter SM, Blau HM, et al. Dermatologist-level
19 782 classification of skin cancer with deep neural networks. *Nature* 2017;542:115–8.
- 20 783 [25] Lotter W, Diab AR, Haslam B, Kim JG, Grisot G, Wu E, et al. Robust breast cancer
21 784 detection in mammography and digital breast tomosynthesis using an annotation-
22 785 efficient deep learning approach. *Nat Med* 2021;27:244–9.
- 23 786 [26] Nikolov S, Blackwell S, Zverovitch A, Mendes R, Livne M, De Fauw J, et al. Deep
24 787 learning to achieve clinically applicable segmentation of head and neck anatomy for
25 788 radiotherapy. *arXiv [csCV]* 2018.
- 26 789 [27] Shen L, Margolies LR, Rothstein JH, Fluder E, McBride R, Sieh W. Deep Learning to
27 790 Improve Breast Cancer Detection on Screening Mammography. *Sci Rep* 2019;9:12495.
- 28 791 [28] Komura D, Ishikawa S. Machine Learning Methods for Histopathological Image
29 792 Analysis. *Computational and Structural Biotechnology Journal* 2018;16:34–42.
30 793 <https://doi.org/10.1016/j.csbj.2018.01.001>.
- 31 794 [29] Yadav SS, Jadhav SM. Deep convolutional neural network based medical image
32 795 classification for disease diagnosis. *Journal of Big Data* 2019;6:113.
- 33 796 [30] Zhang X, Zhao H, Zhang S, Li R. A Novel Deep Neural Network Model for Multi-Label
34 797 Chronic Disease Prediction. *Front Genet* 2019;10:351.
- 35 798 [31] Hesamian MH, Jia W, He X, Kennedy P. Deep Learning Techniques for Medical Image
36 799 Segmentation: Achievements and Challenges. *J Digit Imaging* 2019;32:582–96.
- 37 800 [32] Ibragimov B, Xing L. Segmentation of organs-at-risks in head and neck CT images
38 801 using convolutional neural networks. *Med Phys* 2017;44:547–57.
- 39 802 [33] Javaid U, Souris K, Dasnoy D, Huang S, Lee JA. Mitigating inherent noise in Monte
40 803 Carlo dose distributions using dilated U-Net. *Med Phys* 2019;46:5790–8.
- 41 804 [34] Nguyen D, Long T, Jia X, Lu W, Gu X, Iqbal Z, et al. A feasibility study for predicting
42 805 optimal radiation therapy dose distributions of prostate cancer patients from patient
43 806 anatomy using deep learning. *Sci Rep* 2019;9:1076.
- 44 807 [35] Chen C, Dou Q, Chen H, Qin J, Heng PA. Unsupervised Bidirectional Cross-Modality
45 808 Adaptation via Deeply Synergistic Image and Feature Alignment for Medical Image
46 809 Segmentation. *IEEE Trans Med Imaging* 2020;39:2494–505.
- 47 810 [36] Perone CS, Ballester P, Barros RC, Cohen-Adad J. Unsupervised domain adaptation
48 811 for medical imaging segmentation with self-ensembling. *NeuroImage* 2019;194:1–11.
49 812 <https://doi.org/10.1016/j.neuroimage.2019.03.026>.
- 50 813 [37] Dou Q, Ouyang C, Chen C, Chen H, Glocker B, Zhuang X, et al. PnP-AdaNet: Plug-
51 814 and-Play Adversarial Domain Adaptation Network at Unpaired Cross-Modality Cardiac
52 815 Segmentation. *IEEE Access* 2019;7:99065–76.
53 816 <https://doi.org/10.1109/access.2019.2929258>.
- 54 817 [38] Liu Y, Lei Y, Wang Y, Wang T, Ren L, Lin L, et al. MRI-based treatment planning for
55 818
56 819
57 820
58 821
59 822
60 823
61 824
62
63
64
65

- 818 proton radiotherapy: dosimetric validation of a deep learning-based liver synthetic CT
1 819 generation method. *Phys Med Biol* 2019;64:145015.
- 2 820 [39] Liu Y, Lei Y, Wang T, Fu Y, Tang X, Curran WJ, et al. CBCT-based synthetic CT
3 821 generation using deep-attention cycleGAN for pancreatic adaptive radiotherapy. *Med*
4 822 *Phys* 2020;47:2472–83.
- 5 823 [40] Lei Y, Harms J, Wang T, Liu Y, Shu H, Jani AB, et al. MRI-only based synthetic CT
6 824 generation using dense cycle consistent generative adversarial networks. *Medical*
7 825 *Physics* 2019;46:3565–81. <https://doi.org/10.1002/mp.13617>.
- 8 826 [41] Aganj I, Harisinghani MG, Weissleder R, Fischl B. Unsupervised Medical Image
9 827 Segmentation Based on the Local Center of Mass. *Sci Rep* 2018;8:13012.
- 10 828 [42] Peikari M, Salama S, Nofech-Mozes S, Martel AL. A Cluster-then-label Semi-supervised
11 829 Learning Approach for Pathology Image Classification. *Scientific Reports* 2018;8.
12 830 <https://doi.org/10.1038/s41598-018-24876-0>.
- 13 831 [43] Jin C-B, Kim H, Liu M, Han IH, Lee JI, Lee JH, et al. DC2Anet: Generating Lumbar
14 832 Spine MR Images from CT Scan Data Based on Semi-Supervised Learning. *Applied*
15 833 *Sciences* 2019;9:2521. <https://doi.org/10.3390/app9122521>.
- 16 834 [44] Wang Z, Lin Y, Cheng K-TT, Yang X. Semi-supervised mp-MRI data synthesis with
17 835 StitchLayer and auxiliary distance maximization. *Med Image Anal* 2020;59:101565.
- 18 836 [45] Ge C, Gu IY-H, Jakola AS, Yang J. Deep semi-supervised learning for brain tumor
19 837 classification. *BMC Med Imaging* 2020;20:87.
- 20 838 [46] Burton W 2nd, Myers C, Rullkoetter P. Semi-supervised learning for automatic
21 839 segmentation of the knee from MRI with convolutional neural networks. *Comput*
22 840 *Methods Programs Biomed* 2020;189:105328.
- 23 841 [47] Cheplygina V, de Bruijne M, Pluim JPW. Not-so-supervised: A survey of semi-
24 842 supervised, multi-instance, and transfer learning in medical image analysis. *Med Image*
25 843 *Anal* 2019;54:280–96.
- 26 844 [48] Fréney B, Verleysen M. Classification in the presence of label noise: a survey. *IEEE*
27 845 *Trans Neural Netw Learn Syst* 2014;25:845–69.
- 28 846 [49] Chen T, Kornblith S, Norouzi M, Hinton G. A Simple Framework for Contrastive
29 847 Learning of Visual Representations. In: Iii HD, Singh A, editors. *Proceedings of the 37th*
30 848 *International Conference on Machine Learning*, vol. 119, PMLR; 2020, p. 1597–607.
- 31 849 [50] Zhang J, Wang C, Sheng Y, Palta M, Czito B, Willett C, et al. An interpretable planning
32 850 bot for pancreas stereotactic body radiation therapy. *Int J Radiat Oncol Biol Phys* 2020.
33 851 <https://doi.org/10.1016/j.ijrobp.2020.10.019>.
- 34 852 [51] Shen C, Gonzalez Y, Klages P, Qin N, Jung H, Chen L, et al. Intelligent inverse
35 853 treatment planning via deep reinforcement learning, a proof-of-principle study in high
36 854 dose-rate brachytherapy for cervical cancer. *Phys Med Biol* 2019;64:115013.
- 37 855 [52] Shen C, Nguyen D, Chen L, Gonzalez Y, McBeth R, Qin N, et al. Operating a treatment
38 856 planning system using a deep-reinforcement learning-based virtual treatment planner
39 857 for prostate cancer intensity-modulated radiation therapy treatment planning. *Med Phys*
40 858 *2020;47:2329–36*.
- 41 859 [53] Watts J, Khojandi A, Vasudevan R, Ramdhani R. Optimizing Individualized Treatment
42 860 Planning for Parkinson's Disease Using Deep Reinforcement Learning. *Conf Proc IEEE*
43 861 *Eng Med Biol Soc* 2020;2020:5406–9.
- 44 862 [54] Winkel DJ, Weikert TJ, Breit H-C, Chabin G, Gibson E, Heye TJ, et al. Validation of a
45 863 fully automated liver segmentation algorithm using multi-scale deep reinforcement
46 864 learning and comparison versus manual segmentation. *Eur J Radiol* 2020;126:108918.
- 47 865 [55] Li Z, Xia Y. Deep Reinforcement Learning for Weakly-Supervised Lymph Node
48 866 Segmentation in CT Images. *IEEE J Biomed Health Inform* 2020;PP.
49 867 <https://doi.org/10.1109/JBHI.2020.3008759>.
- 50 868 [56] Thrun S, Pratt L. Learning to Learn: Introduction and Overview. In: Thrun S, Pratt L,
51 869 editors. *Learning to Learn*, Boston, MA: Springer US; 1998, p. 3–17.
- 52 870 [57] Pan SJ, Yang Q. A Survey on Transfer Learning. *IEEE Trans Knowl Data Eng*
53 871 *2010;22:1345–59*.
- 54 872 [58] Zhen X, Chen J, Zhong Z, Hrycushko B, Zhou L, Jiang S, et al. Deep convolutional
55
56
57
58
59
60
61
62
63
64
65

873 neural network with transfer learning for rectum toxicity prediction in cervical cancer
1 874 radiotherapy: a feasibility study. *Phys Med Biol* 2017;62:8246–63.

2 875 [59] Morid MA, Borjali A, Del Fiol G. A scoping review of transfer learning research on
3 876 medical image analysis using ImageNet. *Comput Biol Med* 2021;128:104115.

4 877 [60] Shin H-C, Roth HR, Gao M, Lu L, Xu Z, Nogues I, et al. Deep Convolutional Neural
5 878 Networks for Computer-Aided Detection: CNN Architectures, Dataset Characteristics
6 879 and Transfer Learning. *IEEE Trans Med Imaging* 2016;35:1285–98.

7 880 [61] van Opbroek A, Ikram MA, Vernooij MW, de Bruijne M. Transfer learning improves
8 881 supervised image segmentation across imaging protocols. *IEEE Trans Med Imaging*
9 882 2015;34:1018–30.

10 883 [62] Kandalan RN, Nguyen D, Rezaeian NH, Barragán-Montero AM, Breedveld S, Namuduri
11 884 K, et al. Dose Prediction with Deep Learning for Prostate Cancer Radiation Therapy:
12 885 Model adaptation to Different Treatment Planning Practices. *Radiother Oncol* 2020.
13 886 <https://doi.org/10.1016/j.radonc.2020.10.027>.

14 887 [63] Schapire RE. The strength of weak learnability. 30th Annual Symposium on
15 888 Foundations of Computer Science 1989. <https://doi.org/10.1109/sfcs.1989.63451>.

16 889 [64] Zhang J, Wu QJ, Xie T, Sheng Y, Yin F-F, Ge Y. An Ensemble Approach to Knowledge-
17 890 Based Intensity-Modulated Radiation Therapy Planning. *Front Oncol* 2018;8:57.

18 891 [65] Jia H, Xia Y, Song Y, Cai W, Fulham M, Feng DD. Atlas registration and ensemble deep
19 892 convolutional neural network-based prostate segmentation using magnetic resonance
20 893 imaging. *Neurocomputing* 2018;275:1358–69.
21 894 <https://doi.org/10.1016/j.neucom.2017.09.084>.

22 895 [66] An N, Ding H, Yang J, Au R, Ang TFA. Deep ensemble learning for Alzheimer's disease
23 896 classification. *J Biomed Inform* 2020;105:103411.

24 897 [67] Lan Z, Chen M, Goodman S, Gimpel K, Sharma P, Soricut R. ALBERT: A Lite BERT for
25 898 Self-supervised Learning of Language Representations. *arXiv [csCL]* 2019.

26 899 [68] Devlin J, Chang M-W, Lee K, Toutanova K. BERT: Pre-training of Deep Bidirectional
27 900 Transformers for Language Understanding. *arXiv [csCL]* 2018.

28 901 [69] Conneau A, Khandelwal K, Goyal N, Chaudhary V, Wenzek G, Guzmán F, et al.
29 902 Unsupervised Cross-lingual Representation Learning at Scale. *Proceedings of the 58th*
30 903 *Annual Meeting of the Association for Computational Linguistics* 2020.
31 904 <https://doi.org/10.18653/v1/2020.acl-main.747>.

32 905 [70] Jing L, Tian Y. Self-supervised Visual Feature Learning with Deep Neural Networks: A
33 906 Survey. *IEEE Trans Pattern Anal Mach Intell* 2020;PP.
34 907 <https://doi.org/10.1109/TPAMI.2020.2992393>.

35 908 [71] Kolesnikov A, Zhai X, Beyer L. Revisiting self-supervised visual representation learning.
36 909 *Proceedings of the IEEE/CVF Conference on Computer Vision and Pattern Recognition,*
37 910 2019, p. 1920–9.

38 911 [72] He K, Fan H, Wu Y, Xie S, Girshick R. Momentum contrast for unsupervised visual
39 912 representation learning. *Proceedings of the IEEE/CVF Conference on Computer Vision*
40 913 *and Pattern Recognition, 2020, p. 9729–38.*

41 914 [73] Goyal P, Caron M, Lefaudeaux B, Xu M, Wang P, Pai V, et al. Self-supervised
42 915 Pretraining of Visual Features in the Wild. *arXiv [csCV]* 2021.

43 916 [74] Taleb A, Loetzsch W, Danz N, Severin J, Gaertner T, Bergner B, et al. 3D Self-
44 917 Supervised Methods for Medical Imaging. *arXiv [csCV]* 2020.

45 918 [75] Hatamizadeh A, Yang D, Roth H, Xu D. UNETR: Transformers for 3D Medical Image
46 919 Segmentation. *arXiv [eessIV]* 2021.

47 920 [76] Chen L, Bentley P, Mori K, Misawa K, Fujiwara M, Rueckert D. Self-supervised learning
48 921 for medical image analysis using image context restoration. *Med Image Anal*
49 922 2019;58:101539.

50 923 [77] Nguyen X-B, Lee GS, Kim SH, Yang HJ. Self-Supervised Learning Based on Spatial
51 924 Awareness for Medical Image Analysis. *IEEE Access* 2020;8:162973–81.
52 925 <https://doi.org/10.1109/access.2020.3021469>.

53 926 [78] Han Z, Wei B, Zheng Y, Yin Y, Li K, Li S. Breast Cancer Multi-classification from
54 927 Histopathological Images with Structured Deep Learning Model. *Sci Rep* 2017;7:4172.

- 928 [79] Wang H, Zhou Z, Li Y, Chen Z, Lu P, Wang W, et al. Comparison of machine learning
1 929 methods for classifying mediastinal lymph node metastasis of non-small cell lung cancer
2 930 from F-FDG PET/CT images. *EJNMMI Res* 2017;7:11.
- 3 931 [80] Becker AS, Mueller M, Stoffel E, Marcon M, Ghafoor S, Boss A. Classification of breast
4 932 cancer in ultrasound imaging using a generic deep learning analysis software: a pilot
5 933 study. *Br J Radiol* 2018;91:20170576.
- 6 934 [81] Cheng J-Z, Ni D, Chou Y-H, Qin J, Tiu C-M, Chang Y-C, et al. Computer-Aided
7 935 Diagnosis with Deep Learning Architecture: Applications to Breast Lesions in US
8 936 Images and Pulmonary Nodules in CT Scans. *Sci Rep* 2016;6:24454.
- 9 937 [82] Guo Z, Li X, Huang H, Guo N, Li Q. Deep Learning-Based Image Segmentation on
10 938 Multimodal Medical Imaging. *IEEE Transactions on Radiation and Plasma Medical
11 939 Sciences* 2019;3:162–9. <https://doi.org/10.1109/trpms.2018.2890359>.
- 12 939 [83] Balagopal A, Kazemifar S, Nguyen D, Lin M-H, Hannan R, Owrangi A, et al. Fully
13 940 automated organ segmentation in male pelvic CT images. *Phys Med Biol*
14 941 2018;63:245015.
- 15 942 [84] Javaid U, Dasnoy D, Lee JA. Multi-organ Segmentation of Chest CT Images in
16 943 Radiation Oncology: Comparison of Standard and Dilated UNet. *Advanced Concepts for
17 944 Intelligent Vision Systems* 2018:188–99. https://doi.org/10.1007/978-3-030-01449-0_16.
- 18 945 [85] Moradi S, Oghli MG, Alizadehasl A, Shiri I, Oveisi N, Oveisi M, et al. MFP-Unet: A novel
19 946 deep learning based approach for left ventricle segmentation in echocardiography. *Phys
20 947 Med* 2019;67:58–69.
- 21 948 [86] Nemoto T, Futakami N, Yagi M, Kunieda E, Akiba T, Takeda A, et al. Simple low-cost
22 949 approaches to semantic segmentation in radiation therapy planning for prostate cancer
23 950 using deep learning with non-contrast planning CT images. *Phys Med* 2020;78:93–100.
- 24 951 [87] Nguyen D, Jia X, Sher D, Lin M-H, Iqbal Z, Liu H, et al. 3D radiotherapy dose prediction
25 952 on head and neck cancer patients with a hierarchically densely connected U-net deep
26 953 learning architecture. *Phys Med Biol* 2019;64:065020.
- 27 954 [88] Fan J, Wang J, Chen Z, Hu C, Zhang Z, Hu W. Automatic treatment planning based on
28 955 three-dimensional dose distribution predicted from deep learning technique. *Med Phys*
29 956 2019;46:370–81.
- 30 957 [89] Han X. MR-based synthetic CT generation using a deep convolutional neural network
31 958 method. *Med Phys* 2017;44:1408–19.
- 32 959 [90] Kazemifar S, McGuire S, Timmerman R, Wardak Z, Nguyen D, Park Y, et al. MRI-only
33 960 brain radiotherapy: Assessing the dosimetric accuracy of synthetic CT images
34 961 generated using a deep learning approach. *Radiother Oncol* 2019;136:56–63.
- 35 962 [91] Madani A, Moradi M, Karargyris A, Syeda-Mahmood T. Semi-supervised learning with
36 963 generative adversarial networks for chest X-ray classification with ability of data domain
37 964 adaptation. 2018 IEEE 15th International Symposium on Biomedical Imaging (ISBI
38 965 2018) 2018. <https://doi.org/10.1109/isbi.2018.8363749>.
- 39 966 [92] Jiang J, Hu Y-C, Tyagi N, Rimner A, Lee N, Deasy JO, et al. PSIGAN: Joint Probabilistic
40 967 Segmentation and Image Distribution Matching for Unpaired Cross-Modality Adaptation-
41 968 Based MRI Segmentation. *IEEE Trans Med Imaging* 2020;39:4071–84.
- 42 969 [93] Lynch CM, van Berkel VH, Frieboes HB. Application of unsupervised analysis
43 970 techniques to lung cancer patient data. *PLoS One* 2017;12:e0184370.
- 44 971 [94] Mehta J, Majumdar A. RODEO: Robust DE-aliasing autoencoder for real-time medical
45 972 image reconstruction. *Pattern Recognit* 2017;63:499–510.
- 46 973 [95] Shen C, Gonzalez Y, Chen L, Jiang SB, Jia X. Intelligent Parameter Tuning in
47 974 Optimization-Based Iterative CT Reconstruction via Deep Reinforcement Learning.
48 975 *IEEE Trans Med Imaging* 2018;37:1430–9.
- 49 976 [96] Barkousaraie AS, Bohara G, Jiang SB, Nguyen D. A reinforcement learning application
50 977 of a guided Monte Carlo Tree Search algorithm for beam orientation selection in
51 978 radiation therapy. *Mach Learn: Sci Technol* 2021. [https://doi.org/10.1088/2632-
52 979 2153/abe528](https://doi.org/10.1088/2632-2153/abe528).
- 53 980 [97] Liang X, Chen L, Nguyen D, Zhou Z, Gu X, Yang M, et al. Generating synthesized
54 981 computed tomography (CT) from cone-beam computed tomography (CBCT) using
55 982

- 983 CycleGAN for adaptive radiation therapy. *Phys Med Biol* 2019;64:125002.
- 1 984 [98] Yang X, Lin Y, Wang Z, Li X, Cheng K-T. Bi-Modality Medical Image Synthesis Using
2 985 Semi-Supervised Sequential Generative Adversarial Networks. *IEEE J Biomed Health*
3 986 *Inform* 2020;24:855–65.
- 4 987 [99] Liang X, Nguyen D, Jiang SB. Generalizability issues with deep learning models in
5 988 medicine and their potential solutions: illustrated with cone-beam computed tomography
6 989 (CBCT) to computed tomography (CT) image conversion. *Machine Learning: Science*
7 990 *and Technology* 2020;2:015007. <https://doi.org/10.1088/2632-2153/abb214>.
- 8 991 [100] McIntosh C, Welch M, McNiven A, Jaffray DA, Purdie TG. Fully automated treatment
9 992 planning for head and neck radiotherapy using a voxel-based dose prediction and dose
10 993 mimicking method. *Phys Med Biol* 2017;62:5926–44.
- 11 994 [101] McIntosh C, Purdie TG. Voxel-based dose prediction with multi-patient atlas selection
12 995 for automated radiotherapy treatment planning. *Phys Med Biol* 2017;62:415–31.
- 13 996 [102] Nguyen D, Sadeghnejad Barkousaraie A, Bohara G, Balagopal A, McBeth R, Lin M-
14 997 H, et al. A comparison of Monte Carlo dropout and bootstrap aggregation on the
15 998 performance and uncertainty estimation in radiation therapy dose prediction with deep
16 999 learning neural networks. *Phys Med Biol* 2021;66:054002.
- 17 1000 [103] Valdes G, Luna JM, Eaton E, Simone CB 2nd, Ungar LH, Solberg TD. MediBoost: a
18 1001 Patient Stratification Tool for Interpretable Decision Making in the Era of Precision
19 1002 Medicine. *Sci Rep* 2016;6:37854.
- 20 1003 [104] Lambin P, Leijenaar RTH, Deist TM, Peerlings J, de Jong EEC, van Timmeren J, et
21 1004 al. Radiomics: the bridge between medical imaging and personalized medicine. *Nat Rev*
22 1005 *Clin Oncol* 2017;14:749–62.
- 23 1006 [105] Lambin P, Rios-Velazquez E, Leijenaar R, Carvalho S, van Stiphout RGPM, Granton
24 1007 P, et al. Radiomics: extracting more information from medical images using advanced
25 1008 feature analysis. *Eur J Cancer* 2012;48:441–6.
- 26 1009 [106] Textural Features for Image Classification n.d.
27 1010 <https://doi.org/10.1109%2FTSMC.1973.4309314> (accessed March 29, 2021).
- 28 1011 [107] Jolliffe IT. *Principal Component Analysis*. Springer Science & Business Media; 2013.
- 29 1012 [108] Cristianini N. Fisher Discriminant Analysis (Linear Discriminant Analysis). *Dictionary*
30 1013 *of Bioinformatics and Computational Biology* 2004.
- 31 1014 <https://doi.org/10.1002/9780471650126.dob0238.pub2>.
- 32 1015 [109] Hinton GE, Salakhutdinov RR. Reducing the dimensionality of data with neural
33 1016 networks. *Science* 2006;313:504–7.
- 34 1017 [110] Kohavi R, John GH. The Wrapper Approach. *Feature Extraction, Construction and*
35 1018 *Selection* 1998:33–50. https://doi.org/10.1007/978-1-4615-5725-8_3.
- 36 1019 [111] Guyon I, Gunn S, Nikravesh M, Zadeh LA. *Feature Extraction: Foundations and*
37 1020 *Applications*. Springer; 2008.
- 38 1021 [112] Lal TN, Chapelle O, Weston J, Elisseeff A. Embedded Methods. *Feature Extraction*
39 1022 *n.d.*:137–65. https://doi.org/10.1007/978-3-540-35488-8_6.
- 40 1023 [113] Yang F, Chen W, Wei H, Zhang X, Yuan S, Qiao X, et al. Machine Learning for
41 1024 Histologic Subtype Classification of Non-Small Cell Lung Cancer: A Retrospective
42 1025 Multicenter Radiomics Study. *Front Oncol* 2020;10:608598.
- 43 1026 [114] Liu T, Wu G, Yu J, Guo Y, Wang Y, Shi Z, et al. A mRMRMSRC feature selection
44 1027 method for radiomics approach. 2017 39th Annual International Conference of the IEEE
45 1028 Engineering in Medicine and Biology Society (EMBC) 2017.
46 1029 <https://doi.org/10.1109/embc.2017.8036900>.
- 47 1030 [115] Yuan R, Tian L, Chen J. An RF-BFE algorithm for feature selection in radiomics
48 1031 analysis. *Medical Imaging 2019: Imaging Informatics for Healthcare, Research, and*
49 1032 *Applications* 2019. <https://doi.org/10.1117/12.2512045>.
- 50 1033 [116] Oubel E, Beaumont H, Iannessi A. Mutual information-based feature selection for
51 1034 radiomics. *Medical Imaging 2016: PACS and Imaging Informatics: Next Generation and*
52 1035 *Innovations* 2016. <https://doi.org/10.1117/12.2216746>.
- 53 1036 [117] Wei B-Y, Bing-Yan WEI, Song J-L, Li-Xu GU. The Research of Reproducibility and
54 1037 Non-redundancy Feature Selection Methods in Radiomics. *DEStech Transactions on*

1038 Computer Science and Engineering 2017. <https://doi.org/10.12783/dtcse/aice->
1039 ncs2016/5661.

1040 [118] Sun P, Wang D, Mok VC, Shi L. Comparison of Feature Selection Methods and
1041 Machine Learning Classifiers for Radiomics Analysis in Glioma Grading. *IEEE Access*
1042 2019;7:102010–20. <https://doi.org/10.1109/access.2019.2928975>.

1043 [119] van Timmeren JE, Leijenaar RTH, van Elmpt W, Reymen B, Lambin P. Feature
1044 selection methodology for longitudinal cone-beam CT radiomics. *Acta Oncologica*
1045 2017;56:1537–43. <https://doi.org/10.1080/0284186x.2017.1350285>.

1046 [120] Xu Y, Hosny A, Zeleznik R, Parmar C, Coroller T, Franco I, et al. Deep Learning
1047 Predicts Lung Cancer Treatment Response from Serial Medical Imaging. *Clin Cancer*
1048 *Res* 2019;25:3266–75.

1049 [121] Cybenko G. Approximations by Superpositions of a Sigmoidal Function. 1989.

1050 [122] Hanin B. Universal Function Approximation by Deep Neural Nets with Bounded
1051 Width and ReLU Activations. *Mathematics* 2019;7:992.
1052 <https://doi.org/10.3390/math7100992>.

1053 [123] Erickson BJ, Korfiatis P, Akkus Z, Kline TL. Machine Learning for Medical Imaging.
1054 *Radiographics* 2017;37:505–15.

1055 [124] Hartmann C, Varshney P, Mehrotra K, Gerberich C. Application of information theory
1056 to the construction of efficient decision trees. *IEEE Transactions on Information Theory*
1057 1982;28:565–77. <https://doi.org/10.1109/tit.1982.1056522>.

1058 [125] VAPNIK, V. Pattern recognition using generalized portrait method. *Autom Remote*
1059 *Control* 1963;24:774–80.

1060 [126] Amit Y, Geman D. Shape Quantization and Recognition with Randomized Trees.
1061 *Neural Computation* 1997;9:1545–88. <https://doi.org/10.1162/neco.1997.9.7.1545>.

1062 [127] Breiman L. Random Forests. *Mach Learn* 2001;45:5–32.

1063 [128] Konukoglu E, Glocker B. Random forests in medical image computing. *Handbook of*
1064 *Medical Image Computing and Computer Assisted Intervention*, Elsevier; 2020, p. 457–
1065 80.

1066 [129] Criminisi A, Shotton J, Bucciarelli S. Decision forests with long-range spatial context
1067 for organ localization in CT volumes. *Med Image Comput Comput Assist Interv* 2009.

1068 [130] Lempitsky V, Verhoek M, Noble JA, Blake A. Random Forest Classification for
1069 Automatic Delineation of Myocardium in Real-Time 3D Echocardiography. *Functional*
1070 *Imaging and Modeling of the Heart*, Springer Berlin Heidelberg; 2009, p. 447–56.

1071 [131] Deist TM, Dankers FJWM, Valdes G, Wijsman R, Hsu I-C, Oberije C, et al. Machine
1072 learning algorithms for outcome prediction in (chemo)radiotherapy: An empirical
1073 comparison of classifiers. *Med Phys* 2018;45:3449–59.

1074 [132] Differentiation of glioblastoma from solitary brain metastases using radiomic
1075 machine-learning classifiers. *Cancer Lett* 2019;451:128–35.

1076 [133] Caruana R, Niculescu-Mizil A. An empirical comparison of supervised learning
1077 algorithms. *Proceedings of the 23rd international conference on Machine learning*, New
1078 York, NY, USA: Association for Computing Machinery; 2006, p. 161–8.

1079 [134] Ma C, Wang R, Zhou S, Wang M, Yue H, Zhang Y, et al. The structural similarity
1080 index for IMRT quality assurance: radiomics-based error classification. *Med Phys* 2020.
1081 <https://doi.org/10.1002/mp.14559>.

1082 [135] Akcay M, Etiz D, Celik O. Prediction of Survival and Recurrence Patterns by Machine
1083 Learning in Gastric Cancer Cases Undergoing Radiation Therapy and Chemotherapy.
1084 *Adv Radiat Oncol* 2020;5:1179–87.

1085 [136] Dean JA, Wong KH, Welsh LC, Jones A-B, Schick U, Newbold KL, et al. Normal
1086 tissue complication probability (NTCP) modelling using spatial dose metrics and
1087 machine learning methods for severe acute oral mucositis resulting from head and neck
1088 radiotherapy. *Radiother Oncol* 2016;120:21–7.

1089 [137] Qiu X, Gao J, Yang J, Hu J, Hu W, Kong L, et al. A Comparison Study of Machine
1090 Learning (Random Survival Forest) and Classic Statistic (Cox Proportional Hazards) for
1091 Predicting Progression in High-Grade Glioma after Proton and Carbon Ion
1092 Radiotherapy. *Front Oncol* 2020;10:551420.

1093 [138] Dean J, Wong K, Gay H, Welsh L, Jones A-B, Schick U, et al. Incorporating spatial
11094 dose metrics in machine learning-based normal tissue complication probability (NTCP)
21095 models of severe acute dysphagia resulting from head and neck radiotherapy. *Clin*
31096 *Transl Radiat Oncol* 2018;8:27–39.

41097 [139] Luo Y, Chen S, Valdes G. Machine learning for radiation outcome modeling and
51098 prediction. *Med Phys* 2020;47:e178–84.

61099 [140] Luna JM, Chao H-H, Diffenderfer ES, Valdes G, Chinniah C, Ma G, et al. Predicting
71100 radiation pneumonitis in locally advanced stage II–III non-small cell lung cancer using
81101 machine learning. *Radiotherapy and Oncology* 2019;133:106–12.
101102 <https://doi.org/10.1016/j.radonc.2019.01.003>.

111103 [141] Valdes G, Chang AJ, Interian Y, Owen K, Jensen ST, Ungar LH, et al. Salvage HDR
121104 Brachytherapy: Multiple Hypothesis Testing Versus Machine Learning Analysis. *Int J*
131105 *Radiat Oncol Biol Phys* 2018;101:694–703.

141106 [142] Meti N, Saednia K, Lagree A, Tabbarah S, Mohebpour M, Kiss A, et al. Machine
151107 Learning Frameworks to Predict Neoadjuvant Chemotherapy Response in Breast
161108 Cancer Using Clinical and Pathological Features. *JCO Clin Cancer Inform* 2021;5:66–
171109 80.

191110 [143] Zhou G-Q, Wu C-F, Deng B, Gao T-S, Lv J-W, Lin L, et al. An optimal posttreatment
201111 surveillance strategy for cancer survivors based on an individualized risk-based
211112 approach. *Nature Communications* 2020;11. [https://doi.org/10.1038/s41467-020-17672-](https://doi.org/10.1038/s41467-020-17672-w)
221113 [w](https://doi.org/10.1038/s41467-020-17672-w).

231114 [144] Novak J, Zarinabad N, Rose H, Arvanitis T, MacPherson L, Pinkey B, et al.
241115 Classification of paediatric brain tumours by diffusion weighted imaging and machine
251116 learning. *Sci Rep* 2021;11:2987.

271117 [145] Sheng Y, Li T, Yoo S, Yin F-F, Blitzblau R, Horton JK, et al. Automatic Planning of
281118 Whole Breast Radiation Therapy Using Machine Learning Models. *Front Oncol*
291119 2019;9:750.

301120 [146] McIntosh C, Purdie TG. Contextual Atlas Regression Forests: Multiple-Atlas-Based
311121 Automated Dose Prediction in Radiation Therapy. *IEEE Trans Med Imaging*
321122 2016;35:1000–12.

331123 [147] Babier A, Mahmood R, McNiven AL, Diamant A, Chan TCY. The importance of
341124 evaluating the complete automated knowledge-based planning pipeline. *Phys Med*
351125 2020;72:73–9.

371126 [148] Jog A, Carass A, Roy S, Pham DL, Prince JL. Random forest regression for
381127 magnetic resonance image synthesis. *Med Image Anal* 2017;35:475–88.

391128 [149] Lei Y, Harms J, Wang T, Tian S, Zhou J, Shu H-K, et al. MRI-based synthetic CT
401129 generation using semantic random forest with iterative refinement. *Phys Med Biol*
411130 2019;64:085001.

421131 [150] Yang X, Lei Y, Shu H-K, Rossi P, Mao H, Shim H, et al. Pseudo CT Estimation from
431132 MRI Using Patch-based Random Forest. *Proc SPIE Int Soc Opt Eng* 2017;10133.
441133 <https://doi.org/10.1117/12.2253936>.

451134 [151] Polan DF, Brady SL, Kaufman RA. Tissue segmentation of computed tomography
461135 images using a Random Forest algorithm: a feasibility study. *Phys Med Biol*
471136 2016;61:6553–69.

491137 [152] Gao Y, Shao Y, Lian J, Wang AZ, Chen RC, Shen D. Accurate Segmentation of CT
501138 Male Pelvic Organs via Regression-Based Deformable Models and Multi-Task Random
511139 Forests. *IEEE Trans Med Imaging* 2016;35:1532–43.

521140 [153] Wang T, Lei Y, Fu Y, Curran WJ, Liu T, Nye JA, et al. Machine learning in
531141 quantitative PET: A review of attenuation correction and low-count image reconstruction
541142 methods. *Phys Med* 2020;76:294–306.

551143 [154] Seo H, Badiel Khuzani M, Vasudevan V, Huang C, Ren H, Xiao R, et al. Machine
561144 learning techniques for biomedical image segmentation: An overview of technical
571145 aspects and introduction to state-of-art applications. *Med Phys* 2020;47:e148–67.

591146 [155] Long J, Shelhamer E, Darrell T. Fully convolutional networks for semantic
601147 segmentation. 2015 IEEE Conference on Computer Vision and Pattern Recognition
61
62
63
64
65

- 1148 (CVPR) 2015. <https://doi.org/10.1109/cvpr.2015.7298965>.
- 1149 [156] Ronneberger O, Fischer P, Brox T. U-Net: Convolutional Networks for Biomedical
1150 Image Segmentation. *Medical Image Computing and Computer-Assisted Intervention –*
1151 *MICCAI 2015*, Springer International Publishing; 2015, p. 234–41.
- 1152 [157] Lustberg T, van Soest J, Gooding M, Peressutti D, Aljabar P, van der Stoep J, et al.
1153 Clinical evaluation of atlas and deep learning based automatic contouring for lung
1154 cancer. *Radiother Oncol* 2018;126:312–7.
- 1155 [158] Vrtovec T, Močnik D, Strojjan P, Pernuš F, Ibragimov B. Auto-segmentation of organs
1156 at risk for head and neck radiotherapy planning: From atlas-based to deep learning
1157 methods. *Med Phys* 2020;47:e929–50.
- 1158 [159] König L, Kipshagen T, Rühaak J. A non-linear image registration scheme for real-
1159 time liver ultrasound tracking using normalized gradient fields. *Proc MICCAI CLUST14*,
1160 Boston, USA 2014:29–36.
- 1161 [160] Liu F, Liu D, Tian J, Xie X, Yang X, Wang K. Cascaded one-shot deformable
1162 convolutional neural networks: Developing a deep learning model for respiratory motion
1163 estimation in ultrasound sequences. *Med Image Anal* 2020;65:101793.
- 1164 [161] Raudaschl PF, Zaffino P, Sharp GC, Spadea MF, Chen A, Dawant BM, et al.
1165 Evaluation of segmentation methods on head and neck CT: Auto-segmentation
1166 challenge 2015. *Medical Physics* 2017;44:2020–36. <https://doi.org/10.1002/mp.12197>.
- 1167 [162] Zhu W, Huang Y, Zeng L, Chen X, Liu Y, Qian Z, et al. AnatomyNet: Deep learning
1168 for fast and fully automated whole-volume segmentation of head and neck anatomy.
1169 *Med Phys* 2019;46:576–89.
- 1170 [163] Gou S, Tong N, Qi S, Yang S, Chin R, Sheng K. Self-channel-and-spatial-attention
1171 neural network for automated multi-organ segmentation on head and neck CT images.
1172 *Phys Med Biol* 2020;65:245034.
- 1173 [164] Liang S, Thung K-H, Nie D, Zhang Y, Shen D. Multi-View Spatial Aggregation
1174 Framework for Joint Localization and Segmentation of Organs at Risk in Head and Neck
1175 CT Images. *IEEE Trans Med Imaging* 2020;39:2794–805.
- 1176 [165] Grand Challenge n.d. <https://grand-challenge.org/> (accessed February 17, 2021).
- 1177 [166] Gerard SE, Patton TJ, Christensen GE, Bayouth JE, Reinhardt JM. FissureNet: A
1178 Deep Learning Approach For Pulmonary Fissure Detection in CT Images. *IEEE*
1179 *Transactions on Medical Imaging* 2019;38:156–66.
1180 <https://doi.org/10.1109/tmi.2018.2858202>.
- 1181 [167] Liu P, Dou Q, Wang Q, Heng P-A. An Encoder-Decoder Neural Network With 3D
1182 Squeeze-and-Excitation and Deep Supervision for Brain Tumor Segmentation. *IEEE*
1183 *Access* 2020;8:34029–37. <https://doi.org/10.1109/access.2020.2973707>.
- 1184 [168] Hu H, Li Q, Zhao Y, Zhang Y. Parallel Deep Learning Algorithms with Hybrid
1185 Attention Mechanism for Image Segmentation of Lung Tumors. *IEEE Transactions on*
1186 *Industrial Informatics* 2020:1–1. <https://doi.org/10.1109/tii.2020.3022912>.
- 1187 [169] Zhou T, Ruan S, Guo Y, Canu S. A Multi-Modality Fusion Network Based on
1188 Attention Mechanism for Brain Tumor Segmentation. 2020 IEEE 17th International
1189 Symposium on Biomedical Imaging (ISBI) 2020.
1190 <https://doi.org/10.1109/isbi45749.2020.9098392>.
- 1191 [170] Schlemper J, Oktay O, Schaap M, Heinrich M, Kainz B, Glocker B, et al. Attention
1192 gated networks: Learning to leverage salient regions in medical images. *Med Image*
1193 *Anal* 2019;53:197–207.
- 1194 [171] Jiang H, Gao F, Xu X, Huang F, Zhu S. Attentive and ensemble 3D dual path
1195 networks for pulmonary nodules classification. *Neurocomputing* 2020;398:422–30.
1196 <https://doi.org/10.1016/j.neucom.2019.03.103>.
- 1197 [172] McKinney SM, Sieniek M, Godbole V, Godwin J, Antropova N, Ashrafian H, et al.
1198 International evaluation of an AI system for breast cancer screening. *Nature*
1199 2020;577:89–94.
- 1200 [173] Ibragimov B, Toesca D, Chang D, Yuan Y, Koong A, Xing L. Development of deep
1201 neural network for individualized hepatobiliary toxicity prediction after liver SBRT.
1202 *Medical Physics* 2018;45:4763–74. <https://doi.org/10.1002/mp.13122>.

- 1203 [174] Sekaran K, Chandana P, Murali Krishna N, Kadry S. Deep learning convolutional
11204 neural network (CNN) With Gaussian mixture model for predicting pancreatic cancer.
21205 Multimedia Tools and Applications 2020;79:10233–47. [https://doi.org/10.1007/s11042-](https://doi.org/10.1007/s11042-019-7419-5)
31206 019-7419-5.
- 41207 [175] Barragán-Montero AM, Nguyen D, Lu W, Lin M-H, Norouzi-Kandalan R, Geets X, et
51208 al. Three-dimensional dose prediction for lung IMRT patients with deep neural networks:
61209 robust learning from heterogeneous beam configurations. Medical Physics
71209 2019;46:3679–91. <https://doi.org/10.1002/mp.13597>.
- 81210 [176] Roggen T, Bobic M, Givehchi N, Scheib SG. Deep Learning model for markerless
91211 tracking in spinal SBRT. Phys Med 2020;74:66–73.
- 101212 [177] Mori S, Hirai R, Sakata Y. Simulated four-dimensional CT for markerless tumor
111213 tracking using a deep learning network with multi-task learning. Physica Medica
121214 2020;80:151–8. <https://doi.org/10.1016/j.ejmp.2020.10.023>.
- 131215 [178] Schreier J, Genghi A, Laaksonen H, Morgas T, Haas B. Clinical evaluation of a full-
141216 image deep segmentation algorithm for the male pelvis on cone-beam CT and CT.
151217 Radiother Oncol 2020;145:1–6.
- 161218 [179] Wong J, Fong A, McVicar N, Smith S, Giambattista J, Wells D, et al. Comparing deep
171219 learning-based auto-segmentation of organs at risk and clinical target volumes to expert
181220 inter-observer variability in radiotherapy planning. Radiother Oncol 2020;144:152–8.
- 191221 [180] Gatos I, Tsantis S, Spiliopoulos S, Karnabatidis D, Theotokas I, Zoumpoulis P, et al.
201222 Temporal stability assessment in shear wave elasticity images validated by deep
211223 learning neural network for chronic liver disease fibrosis stage assessment. Med Phys
221224 2019;46:2298–309.
- 231225 [181] Kagadis GC, Drazinos P, Gatos I, Tsantis S, Papadimitroulas P, Spiliopoulos S, et al.
241226 Deep learning networks on chronic liver disease assessment with fine-tuning of shear
251227 wave elastography image sequences. Phys Med Biol 2020;65:215027.
- 261228 [182] Goodfellow I, Pouget-Abadie J, Mirza M, Xu B, Warde-Farley D, Ozair S, et al.
271229 Generative adversarial networks. Communications of the ACM 2020;63:139–44.
281230 <https://doi.org/10.1145/3422622>.
- 291231 [183] Yi X, Walia E, Babyn P. Generative adversarial network in medical imaging: A
301232 review. Med Image Anal 2019;58:101552.
- 311233 [184] Lan L, You L, Zhang Z, Fan Z, Zhao W, Zeng N, et al. Generative Adversarial
321234 Networks and Its Applications in Biomedical Informatics. Front Public Health
331235 2020;8:164.
- 341236 [185] Gonog L, Zhou Y. A Review: Generative Adversarial Networks. 2019 14th IEEE
351237 Conference on Industrial Electronics and Applications (ICIEA), 2019, p. 505–10.
- 361238 [186] Isola P, Zhu J-Y, Zhou T, Efros AA. Image-to-image translation with conditional
371239 adversarial networks. Proceedings of the IEEE conference on computer vision and
381240 pattern recognition, 2017, p. 1125–34.
- 391241 [187] Zhu J-Y, Park T, Isola P, Efros AA. Unpaired Image-to-Image Translation Using
401242 Cycle-Consistent Adversarial Networks. 2017 IEEE International Conference on
411243 Computer Vision (ICCV) 2017. <https://doi.org/10.1109/iccv.2017.244>.
- 421244 [188] Sandfort V, Yan K, Pickhardt PJ, Summers RM. Data augmentation using generative
431245 adversarial networks (CycleGAN) to improve generalizability in CT segmentation tasks.
441246 Sci Rep 2019;9:16884.
- 451247 [189] Shao S, Wang P, Yan R. Generative adversarial networks for data augmentation in
461248 machine fault diagnosis. Computers in Industry 2019;106:85–93.
471249 <https://doi.org/10.1016/j.compind.2019.01.001>.
- 481250 [190] Shorten C, Khoshgoftaar TM. A survey on Image Data Augmentation for Deep
491251 Learning. Journal of Big Data 2019;6. <https://doi.org/10.1186/s40537-019-0197-0>.
- 501252 [191] Maspero M, Savenije MHF, Dinkla AM, Seevinck PR, Intven MPW, Jurgenliemk-
511253 Schulz IM, et al. Dose evaluation of fast synthetic-CT generation using a generative
521254 adversarial network for general pelvis MR-only radiotherapy. Phys Med Biol
531255 2018;63:185001.
- 541256 [192] Wolterink JM, Dinkla AM, Savenije MHF, Seevinck PR, van den Berg CAT, Išgum I.

- 1258 Deep MR to CT Synthesis Using Unpaired Data. *Simulation and Synthesis in Medical*
1259 *Imaging* 2017;14–23. https://doi.org/10.1007/978-3-319-68127-6_2.
- 1260 [193] Kazemifar S, Barragán Montero AM, Souris K, Rivas ST, Timmerman R, Park YK, et
1261 al. Dosimetric evaluation of synthetic CT generated with GANs for MRI-only proton
1262 therapy treatment planning of brain tumors. *J Appl Clin Med Phys* 2020;21:76–86.
- 1263 [194] Kurz C, Maspero M, Savenije MHF, Landry G, Kamp F, Pinto M, et al. CBCT
1264 correction using a cycle-consistent generative adversarial network and unpaired training
1265 to enable photon and proton dose calculation. *Phys Med Biol* 2019;64:225004.
- 1266 [195] Bowles C, Chen L, Guerrero R, Bentley P, Gunn R, Hammers A, et al. GAN
1267 Augmentation: Augmenting Training Data using Generative Adversarial Networks 2018.
- 1268 [196] Qi M, Li Y, Wu A, Jia Q, Li B, Sun W, et al. Multi-sequence MR image-based
1269 synthetic CT generation using a generative adversarial network for head and neck MRI-
1270 only radiotherapy. *Med Phys* 2020;47:1880–94.
- 1271 [197] Liu Y, Lei Y, Wang Y, Shafai-Erfani G, Wang T, Tian S, et al. Evaluation of a deep
1272 learning-based pelvic synthetic CT generation technique for MRI-based prostate proton
1273 treatment planning. *Phys Med Biol* 2019;64:205022.
- 1274 [198] Wang Y, Wang S, Chen J, Wu C. Whole mammographic mass segmentation using
1275 attention mechanism and multiscale pooling adversarial network. *J Med Imaging*
1276 (Bellingham) 2020;7:054503.
- 1277 [199] Rezaei M, Yang H, Meinel C. Recurrent generative adversarial network for learning
1278 imbalanced medical image semantic segmentation. *Multimedia Tools and Applications*
1279 2020;79:15329–48. <https://doi.org/10.1007/s11042-019-7305-1>.
- 1280 [200] Khosravan N, Mortazi A, Wallace M, Bagci U. PAN: Projective Adversarial Network
1281 for Medical Image Segmentation. *Lecture Notes in Computer Science* 2019:68–76.
1282 https://doi.org/10.1007/978-3-030-32226-7_8.
- 1283 [201] Jia H, Xia Y, Song Y, Zhang D, Huang H, Zhang Y, et al. 3D APA-Net: 3D
1284 Adversarial Pyramid Anisotropic Convolutional Network for Prostate Segmentation in
1285 MR Images. *IEEE Trans Med Imaging* 2020;39:447–57.
- 1286 [202] Huo Y, Xu Z, Bao S, Bermudez C, Plassard AJ, Liu J, et al. Splenomegaly
1287 Segmentation using Global Convolutional Kernels and Conditional Generative
1288 Adversarial Networks. *Proc SPIE Int Soc Opt Eng* 2018;10574.
1289 <https://doi.org/10.1117/12.2293406>.
- 1290 [203] Dong X, Lei Y, Wang T, Thomas M, Tang L, Curran WJ, et al. Automatic multiorgan
1291 segmentation in thorax CT images using U-net-GAN. *Med Phys* 2019;46:2157–68.
- 1292 [204] Kearney V, Chan JW, Wang T, Perry A, Descovich M, Morin O, et al. DoseGAN: a
1293 generative adversarial network for synthetic dose prediction using attention-gated
1294 discrimination and generation. *Sci Rep* 2020;10:11073.
- 1295 [205] Babier A, Mahmood R, McNiven AL, Diamant A, Chan TCY. Knowledge-based
1296 automated planning with three-dimensional generative adversarial networks. *Med Phys*
1297 2020;47:297–306.
- 1298 [206] Murakami Y, Magome T, Matsumoto K, Sato T, Yoshioka Y, Oguchi M. Fully
1299 automated dose prediction using generative adversarial networks in prostate cancer
1300 patients. *PLoS One* 2020;15:e0232697.
- 1301 [207] Mahmood R, Babier A, McNiven A, Diamant A, Chan TCY. Automated Treatment
1302 Planning in Radiation Therapy using Generative Adversarial Networks. In: Doshi-Velez
1303 F, Fackler J, Jung K, Kale D, Ranganath R, Wallace B, et al., editors. *Proceedings of*
1304 *the 3rd Machine Learning for Healthcare Conference*, vol. 85, Palo Alto, California:
1305 PMLR; 2018, p. 484–99.
- 1306 [208] Koike Y, Anetai Y, Takegawa H, Ohira S, Nakamura S, Tanigawa N. Deep learning-
1307 based metal artifact reduction using cycle-consistent adversarial network for intensity-
1308 modulated head and neck radiation therapy treatment planning. *Phys Med* 2020;78:8–
1309 14.
- 1310 [209] Schlegl T, Seeböck P, Waldstein SM, Schmidt-Erfurth U, Langs G. *Unsupervised*
1311 *Anomaly Detection with Generative Adversarial Networks to Guide Marker Discovery.*
1312 *Information Processing in Medical Imaging*, Springer International Publishing; 2017, p.

1313 146–57.

11314 [210] Xie X, Niu J, Liu X, Chen Z, Tang S, Yu S. A survey on incorporating domain
21315 knowledge into deep learning for medical image analysis. *Med Image Anal*
31316 2021;69:101985.

41317 [211] Deng C, Ji X, Rainey C, Zhang J, Lu W. Integrating Machine Learning with Human
51318 Knowledge. *iScience* 2020;23:101656.

61319 [212] Nguyen D, McBeth R, Sadeghnejad Barkousaraie A, Bohara G, Shen C, Jia X, et al.
71320 Incorporating human and learned domain knowledge into training deep neural networks:
81321 A differentiable dose-volume histogram and adversarial inspired framework for
91322 generating Pareto optimal dose distributions in radiation therapy. *Med Phys*
101323 2020;47:837–49.

121324 [213] Zhen S-H, Cheng M, Tao Y-B, Wang Y-F, Juengpanich S, Jiang Z-Y, et al. Deep
131325 Learning for Accurate Diagnosis of Liver Tumor Based on Magnetic Resonance Imaging
141326 and Clinical Data. *Front Oncol* 2020;10:680.

151327 [214] Shehata M, Shalaby A, Switala AE, El-Baz M, Ghazal M, Fraiwan L, et al. A
161328 multimodal computer-aided diagnostic system for precise identification of renal allograft
171329 rejection: Preliminary results. *Med Phys* 2020;47:2427–40.

191330 [215] Huang S-C, Pareek A, Seyyedi S, Banerjee I, Lungren MP. Fusion of medical
201331 imaging and electronic health records using deep learning: a systematic review and
211332 implementation guidelines. *NPJ Digit Med* 2020;3:136.

221333 [216] Hu J, Song Y, Wang Q, Bai S, Yi Z. Incorporating historical sub-optimal deep neural
231334 networks for dose prediction in radiotherapy. *Med Image Anal* 2021;67:101886.

241335 [217] Xing Y, Zhang Y, Nguyen D, Lin M-H, Lu W, Jiang S. Boosting radiotherapy dose
251336 calculation accuracy with deep learning. *J Appl Clin Med Phys* 2020;21:149–59.

261337 [218] Kontaxis C, Bol GH, Legendijk JJW, Raaymakers BW. DeepDose: Towards a fast
271338 dose calculation engine for radiation therapy using deep learning. *Phys Med Biol*
281339 2020;65:075013.

301340 [219] Muralidhar N, Islam MR, Marwah M, Karpatne A, Ramakrishnan N. Incorporating
311341 Prior Domain Knowledge into Deep Neural Networks. 2018 IEEE International
321342 Conference on Big Data (Big Data), 2018, p. 36–45.

331343 [220] Luo Y, Tseng H-H, Cui S, Wei L, Ten Haken RK, El Naqa I. Balancing accuracy and
341344 interpretability of machine learning approaches for radiation treatment outcomes
351345 modeling. *BJR Open* 2019;1:20190021.

361346 [221] Reyes M, Meier R, Pereira S, Silva CA, Dahlweid F-M, von Tengg-Kobligk H, et al.
371347 On the Interpretability of Artificial Intelligence in Radiology: Challenges and
381348 Opportunities. *Radiol Artif Intell* 2020;2:e190043.

401349 [222] Murdoch WJ, James Murdoch W, Singh C, Kumbier K, Abbasi-Asl R, Yu B.
411350 Definitions, methods, and applications in interpretable machine learning. *Proceedings of*
421351 *the National Academy of Sciences* 2019;116:22071–80.
431352 <https://doi.org/10.1073/pnas.1900654116>.

441353 [223] Barredo Arrieta A, Díaz-Rodríguez N, Del Ser J, Bennetot A, Tabik S, Barbado A, et
451354 al. Explainable Artificial Intelligence (XAI): Concepts, taxonomies, opportunities and
461355 challenges toward responsible AI. *Inf Fusion* 2020;58:82–115.

481356 [224] Gennatas ED, Friedman JH, Ungar LH, Pirracchio R, Eaton E, Reichmann LG, et al.
491357 Expert-augmented machine learning. *Proc Natl Acad Sci U S A* 2020;117:4571–7.

501358 [225] Barragán-Montero AM, Thomas M, Defraene G, Michiels S, Haustermans K, Lee JA,
511359 et al. Deep learning dose prediction for IMRT of esophageal cancer: The effect of data
521360 quality and quantity on model performance. *Phys Med* 2021;83:52–63.

531361 [226] Blanch MG. Active Deep Learning for Medical Imaging Segmentation. 2017.

541362 [227] Smailagic A, Costa P, Noh HY, Walawalkar D, Khandelwal K, Galdran A, et al.
551363 MedAL: Accurate and Robust Deep Active Learning for Medical Image Analysis. 2018
561364 17th IEEE International Conference on Machine Learning and Applications (ICMLA)
571365 2018. <https://doi.org/10.1109/icmla.2018.00078>.

581366 [228] Kim T, Lee K, Ham S, Park B, Lee S, Hong D, et al. Active learning for accuracy
591367 enhancement of semantic segmentation with CNN-corrected label curations: Evaluation
601367

1368 on kidney segmentation in abdominal CT. *Sci Rep* 2020;10:366.

11369 [229] Larrazabal AJ, Nieto N, Peterson V, Milone DH, Ferrante E. Gender imbalance in
 21370 medical imaging datasets produces biased classifiers for computer-aided diagnosis.
 31371 *Proc Natl Acad Sci U S A* 2020;117:12592–4.

41372 [230] Z O, Obermeyer Z, Powers B, C et al V. Dissecting racial bias in an algorithm used to
 51373 manage the health of populations. *Yearbook of Paediatric Endocrinology* 2020.
 61374 <https://doi.org/10.1530/ey.17.12.7>.

71375 [231] Wilkinson MD, Dumontier M, Aalbersberg IJJ, Appleton G, Axton M, Baak A, et al.
 81376 The FAIR Guiding Principles for scientific data management and stewardship. *Sci Data*
 91377 2016;3:160018.

101378 [232] Kohli MD, Summers RM, Raymond Geis J. Medical Image Data and Datasets in the
 111379 Era of Machine Learning—Whitepaper from the 2016 C-MIMI Meeting Dataset Session.
 121380 *Journal of Digital Imaging* 2017;30:392–9. <https://doi.org/10.1007/s10278-017-9976-3>.

131381 [233] Harvey H, Glocker B. A Standardised Approach for Preparing Imaging Data for
 141382 Machine Learning Tasks in Radiology. *Artificial Intelligence in Medical Imaging*
 151383 2019:61–72. https://doi.org/10.1007/978-3-319-94878-2_6.

161384 [234] Kortensniemi M, Tsapaki V, Trianni A, Russo P, Maas A, Källman H-E, et al. The
 171385 European Federation of Organisations for Medical Physics (EFOMP) White Paper: Big
 181386 data and deep learning in medical imaging and in relation to medical physics profession.
 191387 *Phys Med* 2018;56:90–3.

201388 [235] Sheller MJ, Anthony Reina G, Edwards B, Martin J, Bakas S. Multi-institutional Deep
 211389 Learning Modeling Without Sharing Patient Data: A Feasibility Study on Brain Tumor
 221390 Segmentation. *Brainlesion: Glioma, Multiple Sclerosis, Stroke and Traumatic Brain*
 231391 *Injuries* 2019:92–104. https://doi.org/10.1007/978-3-030-11723-8_9.

241392 [236] Sheller MJ, Edwards B, Anthony Reina G, Martin J, Pati S, Kotrotsou A, et al.
 251393 Federated learning in medicine: facilitating multi-institutional collaborations without
 261394 sharing patient data. *Scientific Reports* 2020;10. <https://doi.org/10.1038/s41598-020-69250-1>.

271395 [237] Chang K, Balachandar N, Lam C, Yi D, Brown J, Beers A, et al. Distributed deep
 281396 learning networks among institutions for medical imaging. *J Am Med Inform Assoc*
 291397 2018;25:945–54.

301398 [238] Prior F, Almeida J, Kathiravelu P, Kurc T, Smith K, Fitzgerald TJ, et al. Open access
 311399 image repositories: high-quality data to enable machine learning research. *Clin Radiol*
 321400 2020;75:7–12.

331401 [239] Challenges n.d. <https://grand-challenge.org/challenges/> (accessed December 3,
 341402 2020).

351403 [240] Prevedello LM, Halabi SS, Shih G, Wu CC, Kohli MD, Chokshi FH, et al. Challenges
 361404 Related to Artificial Intelligence Research in Medical Imaging and the Importance of
 371405 Image Analysis Competitions. *Radiology: Artificial Intelligence* 2019;1:e180031.

381406 [241] Diaz O, Kushibar K, Osuala R, Linardos A, Garrucho L, Igual L, et al. Data
 391407 preparation for artificial intelligence in medical imaging: A comprehensive guide to open-
 401408 access platforms and tools. *Phys Med* 2021;83:25–37.

411409 [242] Menze BH, Jakab A, Bauer S, Kalpathy-Cramer J, Farahani K, Kirby J, et al. The
 421410 Multimodal Brain Tumor Image Segmentation Benchmark (BRATS). *IEEE Trans Med*
 431411 *Imaging* 2015;34:1993–2024.

441412 [243] Babier A, Zhang B, Mahmood R, Moore KL, Purdie TG, McNiven AL, et al.
 451413 OpenKBP: The open-access knowledge-based planning grand challenge. *arXiv*
 461414 *[physics.med-Ph]* 2020.

471415 [244] Callaway E. “It will change everything”: DeepMind’s AI makes gigantic leap in solving
 481416 protein structures. *Nature* 2020. <https://doi.org/10.1038/d41586-020-03348-4>.

491417 [245] Maier-Hein L, Eisenmann M, Reinke A, Onogur S, Stankovic M, Scholz P, et al. Why
 501418 rankings of biomedical image analysis competitions should be interpreted with care. *Nat*
 511419 *Commun* 2018;9:5217.

521420 [246] Reinke A, Eisenmann M, Onogur S, Stankovic M, Scholz P, Full PM, et al. How to
 531421 Exploit Weaknesses in Biomedical Challenge Design and Organization. *Medical Image*
 541422

1423
11424
2
31425
4
5
6
7
8
9
10
11
12
13
14
15
16
17
18
19
20
21
22
23
24
25
26
27
28
29
30
31
32
33
34
35
36
37
38
39
40
41
42
43
44
45
46
47
48
49
50
51
52
53
54
55
56
57
58
59
60
61
62
63
64
65

Computing and Computer Assisted Intervention – MICCAI 2018 2018:388–95.
https://doi.org/10.1007/978-3-030-00937-3_45.